




Cite this: *Toxicol. Res.*, 2017, **6**, 795

## Candidate genes responsible for early key events of phenobarbital-promoted mouse hepatocellular tumorigenesis based on differentiation of regulating genes between wild type mice and humanized chimeric mice†

Ayako Ohara, Yasuhiko Takahashi, Miwa Kondo, Yu Okuda, Shuji Takeda, Masahiko Kushida, Kentaro Kobayashi, Kayo Sumida and Tomoya Yamada \*

Phenobarbital (PB) is a nongenotoxic hepatocellular carcinogen in rodents. PB induces hepatocellular tumors by activating the constitutive androstane receptor (CAR). Some previous research has suggested the possible involvement of epigenetic regulation in PB-promoted hepatocellular tumorigenesis, but the details of its molecular mechanism are not fully understood. In the present study, comprehensive analyses of DNA methylation, hydroxymethylation and gene expression using microarrays were performed in mouse hepatocellular adenomas induced by a single 90 mg kg<sup>-1</sup> intraperitoneal injection dose of diethylnitrosamine (DEN) followed by 500 ppm PB in the diet for 27 weeks. DNA modification and expression of hundreds of genes are coordinately altered in PB-induced mouse hepatocellular adenomas. Of these, gene network analysis showed alterations of CAR signaling and tumor development-related genes. Pathway enrichment analysis revealed that differentially methylated or hydroxymethylated genes belong mainly to pathways involved in development, immune response and cancer cells in contrast to differentially expressed genes belonging primarily to the cell cycle. Furthermore, overlap was evaluated between the genes with altered expression levels with 5-methylcytosine (5mC) and 5-hydroxymethylcytosine (5hmC) alterations in mouse hepatocellular adenoma induced by DEN/PB and the genes with altered expression levels in the liver of CD-1 mice or humanized chimeric mice treated with PB for 7 days. With the integration of transcriptomic and epigenetic approaches, we detected candidate genes responsible for early key events of PB-promoted mouse hepatocellular tumorigenesis. Interestingly, these genes did not overlap with genes altered by the PB treatment of humanized chimeric mice, thus suggesting a species difference between the effects of PB in mouse and human hepatocytes.

Received 5th June 2017,  
Accepted 23rd August 2017

DOI: 10.1039/c7tx00163k

rsc.li/toxicology-research

## Introduction

Phenobarbital (PB) is a nongenotoxic agent which has been shown to produce hepatocellular tumors in rats and mice.<sup>1</sup> PB is considered to increase hepatocellular tumors by activating the CAR and inducing its nuclear translocation.<sup>2,3</sup> In the nucleus, the CAR forms a heterodimer with the retinoid X receptor (RXR) and regulates the expression of downstream genes by binding PB-responsive enhancer modules in their promoters.<sup>4–6</sup> Previous studies have shown that none of the

Car<sup>-/-</sup> mice developed liver tumors, whereas all Car<sup>+/+</sup> mice developed hepatocellular carcinoma and/or adenoma by PB treatment after tumor initiation with a genotoxic carcinogen, diethylnitrosamine (DEN).<sup>7</sup> The potent mouse CAR activator 1,4-bis[2-(3,5-dichloropyridyloxy)]benzene (TCPOBOP) also does not produce liver tumors in mice with or without DEN initiation in Car<sup>-/-</sup> mice.<sup>8</sup>

In recent years, epigenetic modifications associated with gene expression regulation have been notable as important indicators of biological processes and diseases including tumorigenesis. Well-defined mechanisms of epigenetic regulation are DNA modification such as changing cytosine (C) to 5-methylcytosine (5mC) and 5-hydroxymethylcytosine (5hmC).<sup>9–13</sup> The cytosine residues at CpG sites can be methylated to form 5mC in mammalian genomes. Methylated-CpG plays various roles in gene and chromatin regulation, one of which is interaction with other epigenetic modifications and

Environmental Health Science Laboratory, Sumitomo Chemical Co., Ltd., 1-98, 3-Chome, Kasugade-Naka, Konohana-ku, Osaka 554-8558, Japan.

E-mail: yamadat8@sc.sumitomo-chem.co.jp; Fax: +81-66466-5442;

Tel: +81-66466-5322

†Electronic supplementary information (ESI) available. See DOI: 10.1039/c7tx00163k

5mC-specific binding proteins in a coordinated manner which leads to gene repression at the gene promoter. In contrast, 5hmC occurs in DNA demethylation processes. 5mC can be enzymatically oxidized to 5hmC, which can be further oxidized to unmethylated cytosine. The 5hmC levels at gene promoters and enhancers may be partially associated with the transcriptional activation of genes. Several reports have suggested that alterations in 5mC and 5hmC profiles correlate with various diseases including hepatic cancers.<sup>14–18</sup>

Some previous research has suggested the possible involvement of epigenetic regulation in carcinogenic promotion after administration of PB. Exposure to PB in mice globally altered the patterns of both 5mC and 5hmC over the entire genome including promoter regions in liver tissue.<sup>18–23</sup> There were several genes differentially expressed with correlated epigenetic changes and possible associations with carcinogenesis.<sup>23</sup> In addition, 5mC and 5hmC alterations also occurred in PB-elicited tumor tissues of the liver.<sup>18,24–26</sup> At the promoter regions of some genes, decreased 5hmC and increased 5mC were observed in PB-induced mouse liver tumors.<sup>26</sup>

Regarding human relevance of the CAR-mediated MOA in hepatocellular tumor production, numerous publications have mentioned that the CAR-mediated MOA is qualitatively not relevant to humans, based on the lack of the key event of increased cell proliferation in PB-induced hepatocellular tumorigenesis.<sup>3,27–42</sup> PB does not stimulate replicative DNA synthesis in hepatocytes of humanized chimeric mice<sup>39</sup> and in a number of studies does not induce replicative DNA synthesis in cultured human hepatocytes.<sup>31,41,43</sup> Epidemiological reports have also supported the conclusion of no increased risk regarding liver tumors in PB-treated humans.<sup>1,3,44</sup>

In contrast, some studies of PB treatment indicated that PB induces cell cycle transcriptional responses in the humanized CAR<sup>8</sup> and humanized CAR/PXR<sup>45</sup> mouse liver, and, furthermore, that PB-treatment produced liver tumors in the humanized CAR/PXR mouse similar to wild type mice but at a significantly lesser extent than the wild type mice.<sup>46</sup> Schwarz's group indicated that the human relevance of the tumorigenicity of PB through CAR activation remains the subject of an ongoing debate.<sup>37,47–50</sup>

We should recognize that the human receptors of the hCAR/hPXR mouse model are operational in a mouse hepatocyte environment. Although the mouse CAR/PXR has been replaced by that of human, cell proliferation is likely to occur in the same way with wild type mouse since all other genes are those of the original mouse. To enhance the scientific understanding of the human relevance of CAR-mediated liver tumorigenesis, it is necessary to determine the mechanism of action for CAR-mediated liver tumorigenesis. Thus, it is important to determine key molecule(s) (especially in the early phase of treatment) involved in CAR-mediated hepatocellular tumorigenesis in rodents and to investigate its human relevance.

While epigenetics are suggested to be related to PB-mediated liver tumorigenesis,<sup>18–20,22,23,25,26,51</sup> as mentioned above, the present study focused on genes with alterations of DNA methylation and hydroxymethylation with concomitant

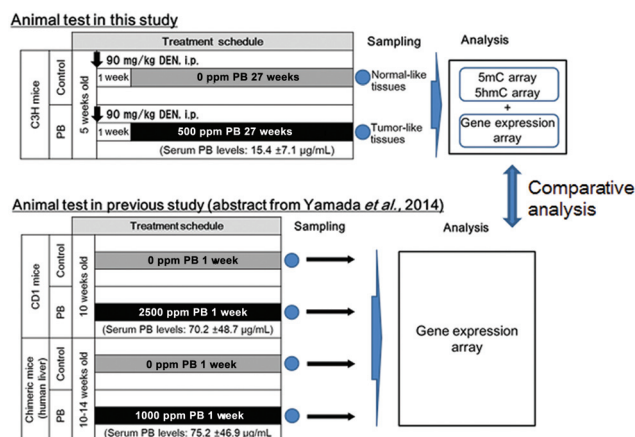


**Fig. 1** Summary of study design for this research. The effects of phenobarbital (PB) on DNA methylation (5mC), DNA hydroxymethylation (5hmC) and gene expression were determined in hepatocellular adenomas induced by DEN/500 ppm PB. Then the altered genes detected in the above analysis were compared to those altered at an early phase of PB treatment in the liver of wild-type mice and chimeric mice with human hepatocytes.<sup>39</sup>

alteration of expression levels. These genes were selected from PB-induced hepatocellular adenomas in mice, by comprehensive analyses of DNA methylation, hydroxymethylation and gene expression using microarrays; we determined the differences in 5mC, 5hmC and transcriptional profiles between hepatocellular adenomas in mice treated with DEN + PB (DEN/500 ppm PB) and control liver samples in age-matched mice treated with DEN alone (DEN/0 ppm PB), and then performed integrated analysis to discover genes with epigenetic and transcriptional correlations (Fig. 1). Using these selected genes, to find the candidates of key genes of CAR-mediated hepatocellular tumorigenesis by transcriptomic and epigenetic approaches in mice, we built gene networks associated with CAR and hepatocellular tumors and investigated pathways enriched for the results. In addition to this, to determine the possible candidates for early key event genes for CAR-mediated MOA of liver tumor formation, the selected genes were evaluated for the overlap of the early altered genes observed in CD-1 mice treated with PB for 7 days.<sup>39</sup> Furthermore, to evaluate its human relevance, the selected early altered genes were also evaluated for the overlap of the altered genes observed in humanized chimeric mice treated with PB for 7 days.<sup>39</sup>

## Materials and methods

### Animals and husbandry

All animal experiments were approved by the Institutional Animal Care and Use Committee at the Environmental Health Science Laboratory of the Sumitomo Chemical Co. Ltd (Approval No. 12-shuyouseibutu-02; 13-shuyouseibutu-02) and were performed in accordance with the Guide for Animal Care and Use at Sumitomo Chemical Co. Ltd. Male C3H/HeNcrCrj mice aged four weeks were purchased from Charles River

Japan, Inc., Hino Breeding Center (Shiga, Japan). Animals were acclimated to laboratory conditions individually for 1 week prior to administration. During the course of the study, the environmental conditions in the animal room were targeted within a temperature range of 22–26 °C and a relative humidity range of 40–70%, with frequent ventilation (more than 10 times per hour) and a 12 h light (8:00–20:00)/12 h dark (20:00–8:00) illumination cycle. One or two animals per cage were housed in suspended aluminum cages with stainless steel wire-mesh fronts and floors (Yamato Scientific Co., Ltd, Tokyo, Japan). A commercially available pulverized diet (CRF-1; Oriental Yeast Co., Ltd, Tokyo) and filtered tap water were provided *ad libitum* throughout the study.

### Study design

The study design is summarized in Fig. 1. Experimental procedures were described previously.<sup>52</sup> Twenty mice were treated with a single intraperitoneal injection of 90 mg per kg bw diethylnitrosamine (DEN, Tokyo Chemical Industry Co., Ltd, Tokyo, Japan; dissolved in saline, 10 ml per kg bw) at 6 weeks before randomly allocating into two groups (ten animals per dose). One week after administration with DEN, diet including sodium phenobarbital (NaPB, referred to as PB in this paper, Wako Pure Chemical Industries, Ltd, Osaka, Japan) at 0 (control) and 500 ppm was administered to each group for 27 weeks. Mortality, body weights, food consumption, PB intake, liver weight, plasma concentration of PB, gross pathology, and liver histopathology (light microscopy) were examined. The animals were sacrificed without fasting by blood withdrawal after decapitation. A part of the liver was fixed in buffered formalin, dehydrated, embedded in paraffin, sectioned, stained with hematoxylin and eosin, and examined by light microscopy. In addition, adjacent parts of the liver sampled for histopathology were stored at –80 °C for gene analysis. The samples of non-neoplastic tissue collected from 3 controls (DEN/0 ppm PB) and neoplastic lesions collected from 3 animals in the PB-treated group (DEN/500 ppm PB) were examined. The plasma concentration of PB was determined by the method previously described.<sup>39</sup>

### DNA and RNA isolation

Genomic DNA and total RNA were isolated using the AllPrep DNA/RNA/miRNA Universal kit (QIAGEN). Liver samples were homogenized and purified with spin columns according to the manufacturer's instructions. The extracted genomic DNA and total RNA were stored at 4 °C and –80 °C, respectively, until just before use.

### 5mC antibody preparation

Mouse monoclonal antibodies to 5mC were generated based on the mouse iliac lymph node method<sup>53</sup> carried out by ITM Co., Ltd. Briefly, the mice were immunized by injecting the tail base with the adjuvant synthetic thiolated 5-methylcytidine. Two weeks later, serum and lymph nodes of the mice were obtained and used for cell fusion of lymph node lymphocytes with a myeloma cell line to make a hybridoma. The resulting

hybridoma cells were cultured onto 96-well plates. The monoclonal antibodies were purified from the positive clone of hybridoma supernatants.

### MeDIP and HmeDIP (5mC and 5hmC immunoprecipitation)

Two µg of genomic DNA from each sample were sonicated to a length between 200–1000 bp using a Q500 Sonicator (Qsonica). Hundred µM Primer-1 and -2 (see ESI Table S1†) were mixed equally, denatured for 5 min at 95 °C and cooled down to room temperature. Sonicated DNA was then end-repaired by incubation for 30 min at 20 °C using the NEBNext End Repair Module (NEB). The reaction mixture was purified using the Agencourt AMPure XP (Beckman Coulter), and subjected to 3'-dA tailing by incubation for 30 min at 37 °C using the NEBNext dA-Tailing Module (NEB). After purification as described above, linker ligation was performed by incubation in a reaction containing 2.5 µM linkers for 1 h at 20 °C using the NEBNext Ultra Ligation Module (NEB). The reaction mixture was purified as described above. Linker-ligated DNA was then denatured for 10 min at 95 °C, followed by cooling rapidly and removing 1% of each sample as input DNA. Denatured DNA (600 ng for MeDIP and 500 ng for HmeDIP) was then immunoprecipitated with each antibody. For MeDIP, 2.1 µg of mouse monoclonal 5mC antibody (as described above) and 10 µl of Magna ChIP™ Protein A + G Magnetic Beads (Millipore) were mixed and incubated overnight at 4 °C in 200 µl of IP buffer (10 mM Tris-HCl, 1 mM EDTA, 1% Triton X-100, 0.1% SDS, 0.1% Na-deoxycholate and 140 mM NaCl). The beads were washed with IP buffer and incubated with denatured DNA overnight at 4 °C in 500 µl of IP buffer. For HmeDIP, denatured DNA and 0.6 µg of rabbit polyclonal 5hmC antibody (Active Motif) were mixed and incubated for 3 h at 4 °C in 500 µl of IP buffer, followed by incubation with 6.3 µl of magnetic beads for 2 h at 4 °C. After immunoprecipitation, the samples were washed with 4 buffers (low salt wash buffer, high salt wash buffer, LiCl wash buffer and TE buffer) (Millipore). Protein was digested with proteinase K (Millipore) overnight at 62 °C. Proteinase K was inactivated by incubating for 10 min at 95 °C. Immunoprecipitated DNA and input DNA were purified as described above, and amplified using Primer-3 (see ESI Table S1†) for 17 cycles in a reaction containing 400 µM dATP, 400 µM dCTP, 400 µM dGTP, 320 µM dTTP, 80 µM dUTP, PfuTurbo Cx Hotstart DNA Polymerase (Agilent Technologies) and 10× reaction buffer. Amplified DNA was purified as described above.

After verification of the specificity of the in-house 5mC antibody, we validated the 5mC- and 5hmC-enriching specificity of MeDIP and HmeDIP in this study based on quantitative PCR analysis for the promoter region of *Cyp2b10* in which the epigenetic alterations by PB exposure up to 13 weeks were reported.<sup>21–23</sup> Statistical significance was determined by Student's *t*-test.

### Quantitative PCR analysis for evaluation of MeDIP and HmeDIP

Primer sequences and their amplified regions for MeDIP and HmeDIP-quantitative PCR are shown in ESI Table S1.† For

quantifying the exon of the Zc3h13 gene, we used Mouse Positive Control Primer Set Zc3h13 (Active Motif). The identity of these target regions in PCR primers was checked using UCSC In-Silico PCR (<http://genome.ucsc.edu/cgi-bin/hgPcr>) and NCBI BLAST (<https://blast.ncbi.nlm.nih.gov/Blast.cgi>). Quantitative PCR assays were performed using a StepOnePlus™ Real-Time PCR System (Applied Biosystems). Immunoprecipitated and input DNA (2 µl of 1/10 diluted) was mixed respectively with Power SYBR Green PCR Master Mix (Applied Biosystems) (15 µl), 10 µM of each pair primers (0.9 µl each) and ultrapure water (11.2 µl). The mixture was incubated for 10 min at 95 °C, and then subjected to PCR reaction for 40 cycles: denatured for 15 s at 95 °C, annealed/extended for 30 s at 68 °C.

### Global DNA methylation and hydroxymethylation analysis

Microarray analysis was conducted on three samples for each group using GeneChip Mouse Promoter 1.0R Arrays (Affymetrix). These arrays contain over 25-mer probes across -7.5 to +2.5 kb from the transcription start site (TSS) of 25 500 mouse promoter regions. The procedure was basically conducted following the manufacturer's protocol (Affymetrix Chromatin Immunoprecipitation Assay Protocol). The obtained image files were analyzed with Partek Genomics Suite 6.6 (Partek). The derived signal values were normalized by quantile normalization and the Robust Multichip Average (RMA) background correlation.<sup>54</sup> These normalized scores were transformed log<sub>2</sub> values and calculated log<sub>2</sub> ratios (MeDIP/input and HmeDIP/input). Signal averages of each group, *p*-values and *t*-values in statistical significance testing (Student's *t*-test) were obtained. The 5mC and 5hmC enriched regions were detected using the Model based Analysis of Tiling-arrays (MAT).<sup>55</sup> MAT algorithm calculated a trimmed mean of the *t*-values of each probe in the window (fragment length = 600 bp, minimum number of probes = 10, top and bottom exclusion = 10%). Using the trimmed mean and the number of probes, MAT scores and the corresponding *p*-values were calculated. All those showing less than 0.01 for the *p*-value were regarded as 5mC/5hmC significantly changed regions. The regions that overlapped within -7.5 to +2.5 kb from the TSS of Refseq genes (mm8) were annotated as the promoters of those genes. We defined the 'promoter' of each gene as the -7.5 kb upstream to +1.5 kb downstream region from the transcription start site (TSS), because the transcription factor binding sites are located mostly in a region upstream to the regulated gene.<sup>56</sup> If 5mC and 5hmC enriched regions by MAT algorithm were overlapped with -7.5 kb to +1.5 kb from the TSS of genes, the regions were annotated with these genes.

### Global gene expression analysis

Gene expression analysis was conducted on three total RNA samples for each group using SurePrint G3 Mouse GE 8 × 60K Microarrays (Agilent Technologies). These arrays contain over 60-mer probes to examine 39 000 mouse mRNAs and 16 000 lncRNAs. The procedure was basically conducted following the

manufacturer's protocol (version 6.5). The scanned image files were converted to TIFF files containing signal values of each probe using Feature Extraction (version 10.7.3.1). The signal values were log<sub>2</sub>-transformed and processed to the 75<sup>th</sup> percentile normalization.<sup>57</sup> Signal averages for each group and the *p*-value in statistical significance testing (Student's *t*-test) were obtained. All those showing less than 0.05 for the *p*-value and "1 (present: gIsPosAndSignif)" for Detection Call in PB-treatment arrays were regarded as up-regulated probe sets. All those showing less than 0.05 for the *p*-value and "1 (present: gIsPosAndSignif)" for Detection Call in the control arrays were regarded as down-regulated probe sets.

### Integrated pathway analysis of 5mC, 5hmC and gene expression

Gene network analyses and pathway enrichment analyses were performed using MetaCore® via <https://portal.genego.com>. For gene network analyses, we used known interaction information with direction (incoming/outgoing), effect (activation/inhibition) and mechanism (*e.g.* bind/influence on expression/transcription regulation) of the CAR and CAR/RXR-alpha complex, followed by using known information of causal associations of genes with liver neoplasms in epigenetic, transcriptional or protein levels. The detailed information and references are shown in the MetaCore website. For pathway analyses, we used known canonical pathways of common functional themes in the MetaCore database and performed the analyses based on the gene list of 5mC, 5hmC and gene expression alterations.

## Results

### Animal data

Although one animal of the DEN/500 ppm PB group was found dead at day 100, treatment with 500 ppm PB did not affect body weight, body weight gain, or food consumption, demonstrating that treatment with 500 ppm PB (average PB intake was 69.9 mg kg<sup>-1</sup> day<sup>-1</sup>) did not show excess toxicity under the present study conditions. Absolute and relative liver weights were significantly increased to 1.4- and 1.5-fold of control, respectively. Histopathological examination revealed that DEN/500 ppm PB induced hepatocellular adenomas in all animals (19/19, *vs.* 7/20 in DEN/0 ppm PB) and adenocarcinomas in some (3/19, *vs.* 0/20 in DEN/0 ppm PB). These data are presented in ESI Tables S2 and S3.† Group mean and standard deviation of plasma concentration of PB in DEN/500 ppm PB was 15.4 ± 7.1 µg mL<sup>-1</sup> (*N* = 19).

### Global profiles of 5mC and 5hmC are altered in mouse hepatocellular adenoma induced by DEN/PB

Normal appearing tissues in 3 animals of the DEN/0 ppm PB group and tissues with hepatocellular adenomas in 3 animals of the DEN/500 ppm PB group were used for global analyses (ESI Table S4 and Fig. S1†). First, we verified the specificity of the in-house 5mC antibody (ESI Fig. S2†). Next, we validated

the 5mC- and 5hmC-enriching specificity of MeDIP and HmeDIP in this study (Fig. 2). We performed quantitative PCR analysis and confirmed that the region without CpG sites was not detected in immunoprecipitated DNA with either 5mC or 5hmC antibodies. As for the promoter region of *Cyp2b10*, both the detected 5mC and 5hmC levels differed between immunoprecipitated DNA of PB-induced tumors in the DEN/500 ppm PB group and control tissues in the DEN/0 ppm PB group. These experiments showed that MeDIP and HmeDIP could specifically enrich 5mC- and 5hmC-containing regions, respectively.

We studied differential epigenetic and expression profiles between tumors of PB-treated mice and normal tissues of control mice by global analyses using microarrays. The 5mC analysis showed significantly hyper- and hypomethylated gene promoters (3594 and 3573) in liver tumors compared to control tissue (Fig. 3). 4980 and 6348 gene promoters were hyper- and hypohydroxymethylated, respectively. Tables 1 and 2 show the top 10 significant differential gene promoters (these regions are arranged in ascending order of *p*-value and MAT-score). With

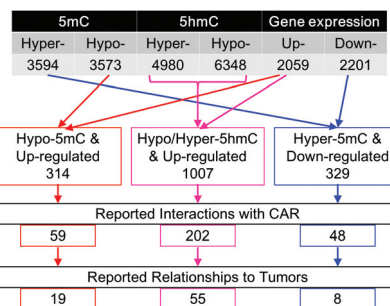


**Fig. 3** Summary results of 5mC, 5hmC and gene expression analysis. These genes were significantly altered in hepatocellular adenoma of mice in the DEN/500 ppm PB group compared to normal livers of control mice in the DEN/0 ppm PB group. We used the MetaCore database to search interactions with CAR and relationships to tumor production.

regard to gene expression, 2059 and 2201 genes were up- and down-regulated, respectively. We also compared the gene expression profile to RNA-sequence data in a previous study

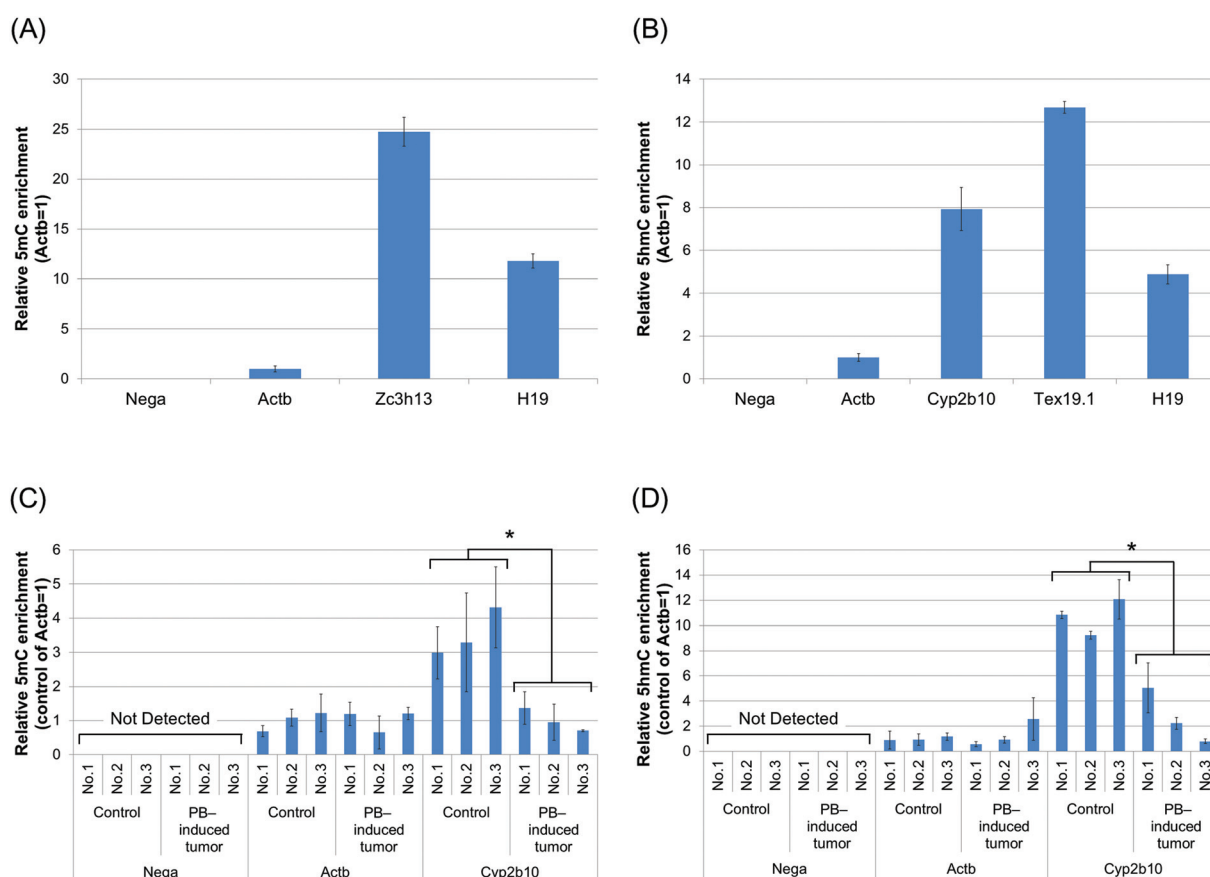


**Fig. 2** Validation of the 5mC- and 5hmC-enriching specificity of MeDIP and HmeDIP in this study. (A, B) Followed by removing 1% of DNA as the input sample, genomic DNA from liver samples of normal control mice was subjected to MeDIP (A) and HmeDIP (B). Immunoprecipitated and input DNA were analyzed by quantitative PCR with primers for the region without CpG sites (Nega), the promoter region of *Actb* (low-level 5mC and 5hmC), *Tex19.1* (high-level 5hmC), *Cyp2b10*, the exon of *Zc3h13* (high-level 5mC) and the imprinting control region of *H19* (high-level 5mC and 5hmC) (ESI Table S1†). (C, D) Likewise, genomic DNA from control tissues (DEN/0 ppm PB) and PB-induced hepatocellular adenoma (DEN/500 ppm PB) was subjected to MeDIP (C) and HmeDIP (D), followed by quantitative PCR with primers as described above for Nega, *Actb* and *Cyp2b10* (known 5mC and 5hmC alteration by PB treatment). Data are mean  $\pm$  SD from triplicate experiments. \**p* < 0.01, Student's *t*-test.

**Table 1** Top 10 most hyper- and hypomethylated gene promoters in hepatocellular tumors of PB-treated mice

[Hypermethylated]							
Gene symbol	Distance to TSS	Chromosome	Region start	Region end	Probes in region	<i>p</i> -Value	MAT-score <sup>a</sup>
Ccnf	-4052	chr17	23983062	23984925	43	$8.83 \times 10^{-6}$	7.038
Prr23a	855	chr9	98652794	98653962	21	$8.83 \times 10^{-6}$	6.485
Oxct2a	0	chr4	122824723	122826092	38	$8.83 \times 10^{-6}$	6.241
Calml3	0	chr13	3802864	3803753	25	$8.83 \times 10^{-6}$	6.217
Zrsr1	1249	chr11	22873278	22874439	28	$8.83 \times 10^{-6}$	6.171
Pcdh12	-1023	chr18	38411399	38412806	35	$8.83 \times 10^{-6}$	6.109
Slc9a1	522	chr4	132642370	132643661	36	$8.83 \times 10^{-6}$	6.076
Donson	0	chr16	91577392	91578500	29	$8.83 \times 10^{-6}$	5.792
5830415F09Rik	453	chr4	46408754	46410071	27	$8.83 \times 10^{-6}$	5.788
Olfr105	-1015	chr17	36988619	36989545	26	$1.77 \times 10^{-5}$	5.705
[Hypomethylated]							
Gene symbol	Distance to TSS	Chromosome	Region start	Region end	Probes in region	<i>p</i> -Value	MAT-score <sup>a</sup>
Psen2	1221	chr1	182080643	182081405	15	$8.83 \times 10^{-6}$	-9.763
Pld3	-3530	chr7	27265403	27266148	18	$8.83 \times 10^{-6}$	-9.475
2310022A10Rik	-3088	chr7	27265403	27266148	18	$8.83 \times 10^{-6}$	-9.475
LOC100041223	0	chrY_random	12134681	12136488	83	$8.83 \times 10^{-6}$	-9.082
LOC100039810	936	chrY_random	12134681	12136488	83	$8.83 \times 10^{-6}$	-9.082
LOC100041256	936	chrY_random	12134681	12136488	83	$8.83 \times 10^{-6}$	-9.082
Pusl1	-5213	chr4	154740776	154741472	19	$8.83 \times 10^{-6}$	-8.317
LOC100042428	0	chrY_random	11615565	11617305	80	$8.83 \times 10^{-6}$	-8.192
MGC107098	1267	chrY_random	11615565	11617305	80	$8.83 \times 10^{-6}$	-8.192
LOC100039753	1285	chrY_random	11615565	11617305	80	$8.83 \times 10^{-6}$	-8.192

<sup>a</sup>The relative methylation level calculated by the MAT (Model based Analysis of Tiling-arrays) algorithm.

**Table 2** Top 10 most hyper- and hypohydroxymethylated gene promoters in hepatocellular tumors of PB-treated mice

[Hyperhydroxymethylated]							
Gene symbol	Distance to TSS	Chromosome	Region start	Region end	Probes in region	<i>p</i> -Value	MAT-score <sup>a</sup>
Mir1982	-479	chr10	80230053	80231447	38	$8.83 \times 10^{-6}$	10.373
Gm9786	228	chr10	80230053	80231447	38	$8.83 \times 10^{-6}$	10.373
Oaz1	268	chr10	80230053	80231447	38	$8.83 \times 10^{-6}$	10.373
LOC100041223	-2138	chrY_random	12131429	12133005	65	$8.83 \times 10^{-6}$	10.228
LOC100039810	-740	chrY_random	12131429	12133005	65	$8.83 \times 10^{-6}$	10.228
LOC100041256	-740	chrY_random	12131429	12133005	65	$8.83 \times 10^{-6}$	10.228
Igfbp5	-320	chr1	72808393	72809533	29	$8.83 \times 10^{-6}$	10.170
C030023E24Rik	-4736	chrX	57444031	57447222	82	$8.83 \times 10^{-6}$	9.465
Cdr1	0	chrX	57444031	57447222	82	$8.83 \times 10^{-6}$	9.465
Trim32	0	chr4	65091192	65092726	40	$8.83 \times 10^{-6}$	9.444
[Hypohydroxymethylated]							
Gene symbol	Distance to TSS	Chromosome	Region start	Region end	Probes in region	<i>p</i> -Value	MAT-score <sup>a</sup>
2210021J22Rik	-2995	chr15	85642459	85645379	81	$8.83 \times 10^{-6}$	-13.554
Hspa1a	-4679	chr17	34584892	34587462	67	$8.83 \times 10^{-6}$	-12.096
Lsm2	-2724	chr17	34584892	34587462	67	$8.83 \times 10^{-6}$	-12.096
Gstt3	-1851	chr10	75226982	75227939	22	$8.83 \times 10^{-6}$	-12.018
Eid3	0	chr10	82296212	82297783	41	$8.83 \times 10^{-6}$	-11.725
Stk40	-5130	chr4	125599936	125601131	34	$8.83 \times 10^{-6}$	-11.623
Lsm10	979	chr4	125599936	125601131	34	$8.83 \times 10^{-6}$	-11.623
Emg1	-1464	chr6	124679262	124682316	79	$8.83 \times 10^{-6}$	-11.309
Phb2	1354	chr6	124679262	124682316	79	$8.83 \times 10^{-6}$	-11.309
BC021614	542	chr19	4057119	4058753	41	$8.83 \times 10^{-6}$	-11.135

<sup>a</sup>The relative methylation level calculated by the MAT (Model based Analysis of Tiling-arrays) algorithm.

focusing on PB-induced liver tumors,<sup>26</sup> and confirmed some reproducibility between these datasets (ESI Fig. S3†).

In some cases, a certain correlation was found between DNA methylation and gene expression. DNA methylation of gene promoter regions is possibly associated with transcriptional repression of some genes, while hydroxymethylated DNA was associated with transcriptional activation.<sup>10–13</sup> To identify the candidates important for PB-mediated hepatocellular tumorigenesis from the thousands of altered genes described above, we integrated 5mC/5hmC and gene expression analyses and focused on these epigenetic and transcriptional correlations. In hepatocellular adenomas developing after PB treatment (DEN/500 ppm PB), 314 genes were up-regulated and hypomethylated, 1007 genes were up-regulated and differentially hydroxymethylated, and 329 genes were down-regulated and hypermethylated compared to control (DEN/0 ppm PB) (Fig. 3).

#### Gene network analysis shows possible interactions with CAR and relationships to liver tumor production in mouse hepatocellular adenoma induced by DEN/PB

To examine whether differential genes in DNA methylation and gene expression are associated with the CAR, we then investigated gene networks using the MetaCore database. In MetaCore, CAR's downstream transcription factors (HNF4-alpha, ESR1 and HIF1A) are reported to interact with many genes of integrated analysis results. We defined these transcription factors as 'hub' genes, and we identified genes that have interaction information of the CAR or its hub genes. In epigenetically and transcriptionally changed genes (up-regulated and hypomethylated; up-regulated and differentially hydroxymethylated; down-regulated and hypermethylated), 59, 202 and 48 genes were reported to have a possible interaction with the CAR or its downstream hub genes, respectively (Fig. 3).

We further investigated associations of our data with liver tumor production-related genes. As a result of analyzing the information on disease, we found that dozens of genes focused above were reported to have causal relationships to liver neoplasms. Fig. 3 shows the number of significantly differential genes that have possible interactions with the CAR and relate to liver tumor production, and Table 3 shows the details of these genes. As for differentially hydroxymethylated and up-regulated genes, both MAT-scores of hyper- and hypohydroxymethylated promoter regions are shown here. Using our data shown in Table 3, we built whole gene networks including the CAR and its downstream hub genes (Fig. 4).

#### Some cancer-related pathways enriched for the results of 5mC, 5hmC and gene expression analyses in mouse hepatocellular adenoma induced by DEN/PB

Next, we performed pathway enrichment analysis using MetaCore pathways and the number of detected pathways by PB administration ( $p < 0.01$ ) for 5mC, 5hmC and gene expression alterations were 288, 366 and 231, respectively (data not shown). Tables 4–6 show the results of the top 20 enriched pathways for genes that were significantly changed in 5mC, 5hmC or gene expression by PB administration, respectively

(these pathways are arranged in ascending order by  $p$ -value). The differentially methylated genes belonged mainly to pathways involved in the development and immune response, such as oncostatin M signaling, megakaryopoiesis, growth hormone signaling and inflammatory response. The main signaling cascades of ovarian cancer are also enriched. The differentially hydroxymethylated genes belonged mainly to pathways involved in development and cancer cells, such as PIP3 (phosphatidylinositol 3,4,5-trisphosphate) signaling, regulation of EMT (epithelial-to-mesenchymal transition), myeloma cells and colorectal cancer. Both changes in 5mC and 5hmC profiles correlated most closely with TGF, WNT and cytoskeletal remodeling. Meanwhile, the differentially expressed genes were intimately related to pathways involved in the cell cycle or immune response such as G1/S transition, the metaphase checkpoint and IL-4-induced regulators of cell growth.

#### Evaluation of overlap between the altered genes at expression levels with 5mC and 5hmC alterations in mouse hepatocellular adenoma induced by DEN/PB and altered genes at expression levels in liver of CD-1 mice and humanized chimeric mice treated with PB for 7 days

To evaluate the possible candidates of early phase marker genes for liver tumorigenesis by the CAR-mediated MOA, we determined overlap between the genes with altered expression levels with 5mC and 5hmC alterations in mouse hepatocellular adenoma induced by DEN/500 ppm PB and the genes previously determined with altered expression levels in the liver of CD-1 mice treated with 2500 ppm PB for 7 days.<sup>39</sup> Several genes with altered expression levels with epigenetic alterations in hepatocellular adenoma induced by DEN/500 ppm PB changed in the same manner (increased or decreased expression levels) in the liver of CD-1 mice treated with 2500 ppm PB for 7 days (Fig. 5, ESI Tables S5–7†). Some of these overlapped genes (Abcc4, Apoa1, Cblb, Ccdc85b, Cdk5r1, Dlg1, Egfr, Prg4 and Tff1) were associated with Gene Ontology (GO) terms related to CAR or beta-catenin and cell proliferation and/or cell growth, and these nine genes previously demonstrated these relationships (Table 7). Furthermore, the overlap between the altered genes at expression levels with 5mC and/or 5hmC alterations in mouse hepatocellular adenoma induced by DEN/500 ppm PB and the altered genes at expression levels of liver in humanized chimeric mice treated with 1000 ppm PB for 7 days, previously determined,<sup>39</sup> was also analyzed. While several genes overlapped, none of the genes related to cell proliferation and/or cell growth overlapped (Fig. 5, ESI Tables S5–7†).

## Discussion

### Candidate key genes for a mode of action involving activation of the constitutive androstane receptor (CAR) in mouse hepatocellular tumorigenesis

We analyzed 5mC, 5hmC and gene expression profiles globally in PB-induced hepatocellular adenomas in mice. Since we

Table 3 Genes reported having interactions with CAR and relationships to tumors

[Hypo-5mC & upregulated]						
Gene symbol	Hypo-5mC		Upregulated			
	<i>p</i> -Value	MAT-score <sup>a</sup>	<i>p</i> -Value		Fold-change	
Abcc2	$9.90 \times 10^{-3}$	-3.069	$7.55 \times 10^{-5}$		2.234	
Afp	$9.68 \times 10^{-3}$	-3.080	$2.80 \times 10^{-2}$		13.655	
Anxa2	$9.34 \times 10^{-3}$	-3.097	$4.43 \times 10^{-2}$		6.270	
Bmp7	$9.59 \times 10^{-3}$	-3.085	$1.39 \times 10^{-3}$		5.299	
Ccne1	$8.77 \times 10^{-3}$	-3.126	$7.11 \times 10^{-4}$		4.063	
Cyr61	$2.05 \times 10^{-3}$	-3.749	$4.09 \times 10^{-2}$		5.303	
Dsc2	$6.04 \times 10^{-3}$	-3.292	$2.31 \times 10^{-2}$		1.293	
Eif4ebp1	$6.29 \times 10^{-3}$	-3.277	$4.47 \times 10^{-3}$		1.250	
F3	$8.20 \times 10^{-3}$	-3.157	$1.39 \times 10^{-3}$		2.831	
Glul	$5.16 \times 10^{-3}$	-3.362	$7.97 \times 10^{-4}$		9.049	
Irs1	$9.30 \times 10^{-3}$	-3.100	$3.31 \times 10^{-3}$		2.714	
Itga6	$9.44 \times 10^{-3}$	-3.094	$2.32 \times 10^{-3}$		2.933	
Junb	$6.50 \times 10^{-3}$	-3.258	$5.47 \times 10^{-3}$		3.254	
Mcm2	$4.41 \times 10^{-5}$	-5.577	$3.20 \times 10^{-2}$		2.721	
Mki67	$5.71 \times 10^{-3}$	-3.315	$1.06 \times 10^{-3}$		21.397	
Nfe2l2	$6.00 \times 10^{-3}$	-3.294	$3.66 \times 10^{-2}$		2.299	
Nlk	$5.68 \times 10^{-3}$	-3.317	$5.06 \times 10^{-3}$		3.764	
Nqo1	$9.25 \times 10^{-3}$	-3.101	$3.39 \times 10^{-4}$		6.660	
Ptp4a3	$7.69 \times 10^{-3}$	-3.184	$3.00 \times 10^{-2}$		2.064	
[Hyper or Hypo-5hmC & upregulated]						
Gene symbol	Hyper-5hmC		Hypo-5hmC		Upregulated	
	<i>p</i> -Value	MAT-score <sup>a</sup>	<i>p</i> -Value	MAT-score <sup>a</sup>	<i>p</i> -Value	Fold-change
Abcc3	—	—	$8.83 \times 10^{-6}$	-7.846	$1.28 \times 10^{-2}$	1.537
Abcc4	$2.33 \times 10^{-3}$	4.113	—	—	$8.93 \times 10^{-5}$	104.220
Aldoa	$6.31 \times 10^{-3}$	3.604	—	—	$2.40 \times 10^{-3}$	1.426
Anxa2	—	—	$1.85 \times 10^{-4}$	-5.126	$4.43 \times 10^{-2}$	6.270
Ar	$2.26 \times 10^{-3}$	4.128	—	—	$4.87 \times 10^{-2}$	1.637
Bak1	—	—	$6.49 \times 10^{-3}$	-3.634	$1.33 \times 10^{-2}$	1.861
Bax	—	—	$7.94 \times 10^{-5}$	-5.403	$4.47 \times 10^{-2}$	1.699
Bcl2 l1	—	—	$1.24 \times 10^{-3}$	-4.429	$1.30 \times 10^{-2}$	1.855
Bmp7	—	—	$1.59 \times 10^{-4}$	-5.204	$1.39 \times 10^{-3}$	5.299
Cd151	—	—	$3.53 \times 10^{-5}$	-5.622	$3.28 \times 10^{-3}$	1.255
Cd44	$2.68 \times 10^{-3}$	4.043	—	—	$3.57 \times 10^{-2}$	4.191
Cd82	—	—	$9.21 \times 10^{-3}$	-3.452	$1.08 \times 10^{-3}$	1.395
Cdc25a	—	—	$5.19 \times 10^{-3}$	-3.739	$2.31 \times 10^{-2}$	1.572
Cdh2	$8.76 \times 10^{-3}$	3.461	$7.91 \times 10^{-3}$	-3.534	$3.76 \times 10^{-2}$	1.706
Cdk2	$9.50 \times 10^{-3}$	3.414	—	—	$2.92 \times 10^{-2}$	1.580
Cdkn1b	—	—	$5.38 \times 10^{-4}$	-4.736	$1.20 \times 10^{-2}$	1.271
Cks1b	$2.82 \times 10^{-4}$	5.052	—	—	$1.60 \times 10^{-2}$	2.038
Cx3cr1	$6.36 \times 10^{-3}$	3.597	—	—	$3.14 \times 10^{-2}$	1.938
Cyr61	$2.67 \times 10^{-3}$	4.046	$1.85 \times 10^{-4}$	-5.144	$4.09 \times 10^{-2}$	5.303
Dlk1	$5.66 \times 10^{-3}$	3.656	—	—	$1.29 \times 10^{-3}$	24.247
Dnmt3a	$8.55 \times 10^{-3}$	3.472	$2.96 \times 10^{-3}$	-4.005	$3.11 \times 10^{-3}$	2.316
Egln2	$2.70 \times 10^{-3}$	4.040	$8.83 \times 10^{-6}$	-7.145	$3.32 \times 10^{-3}$	1.194
Egr1	$7.57 \times 10^{-3}$	3.524	$8.83 \times 10^{-6}$	-6.222	$1.67 \times 10^{-2}$	5.828
Eif4ebp1	—	—	$6.74 \times 10^{-3}$	-3.618	$4.47 \times 10^{-3}$	1.250
Ephx1	—	—	$1.65 \times 10^{-3}$	-4.273	$4.95 \times 10^{-4}$	2.227
Ets2	—	—	$1.47 \times 10^{-3}$	-4.326	$2.01 \times 10^{-2}$	2.590
Ezh2	$6.31 \times 10^{-3}$	3.604	—	—	$4.61 \times 10^{-2}$	2.018
F3	$8.79 \times 10^{-3}$	3.458	$3.88 \times 10^{-4}$	-4.828	$1.39 \times 10^{-3}$	2.831
Fbln1	$9.27 \times 10^{-4}$	4.543	$1.60 \times 10^{-3}$	-4.295	$6.48 \times 10^{-4}$	24.599
Flt1	—	—	$7.29 \times 10^{-3}$	-3.579	$1.93 \times 10^{-2}$	1.718
Foxm1	—	—	$7.90 \times 10^{-3}$	-3.534	$6.99 \times 10^{-3}$	8.387
Glul	—	—	$8.83 \times 10^{-6}$	-6.114	$7.97 \times 10^{-4}$	9.049
H19	$4.93 \times 10^{-3}$	3.724	—	—	$1.65 \times 10^{-3}$	118.119
H2afx	—	—	$8.83 \times 10^{-6}$	-6.041	$1.41 \times 10^{-2}$	2.360
Hmgbl1	$6.34 \times 10^{-3}$	3.600	—	—	$1.90 \times 10^{-2}$	1.263
Irs1	—	—	$2.47 \times 10^{-4}$	-5.032	$3.31 \times 10^{-3}$	2.714
Krt19	$7.50 \times 10^{-3}$	3.529	—	—	$1.08 \times 10^{-2}$	7.442
Mat2a	$5.45 \times 10^{-3}$	3.671	—	—	$2.80 \times 10^{-3}$	3.061
Mcm2	$1.77 \times 10^{-4}$	5.288	$9.68 \times 10^{-3}$	-3.426	$3.20 \times 10^{-2}$	2.721



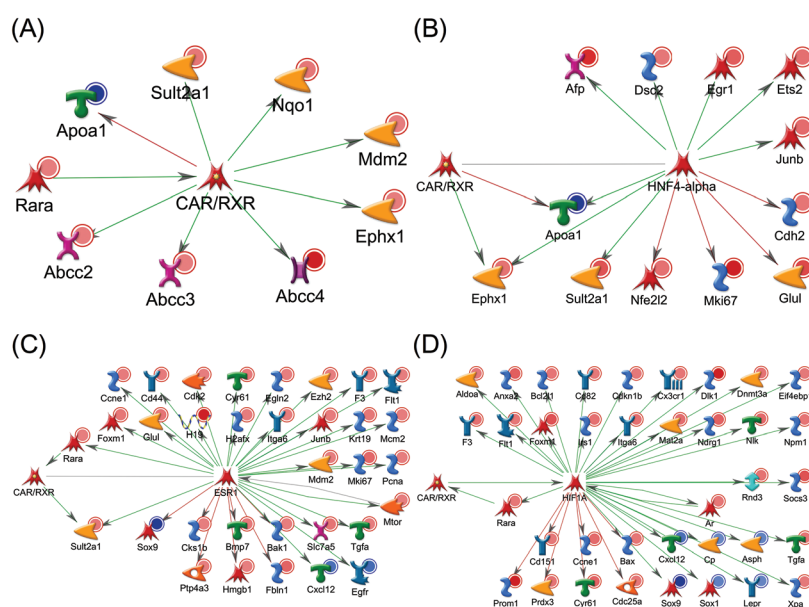
Table 3 (Contd.)

[Hyper or Hypo-5hmC & upregulated]						
Gene symbol	Hyper-5hmC		Hypo-5hmC		Upregulated	
	<i>p</i> -Value	MAT-score <sup>a</sup>	<i>p</i> -Value	MAT-score <sup>a</sup>	<i>p</i> -Value	Fold-change
Mdm2	—	—	$1.47 \times 10^{-3}$	-4.322	$1.09 \times 10^{-2}$	1.511
Mtor	$7.59 \times 10^{-4}$	4.620	—	—	$2.81 \times 10^{-2}$	1.504
Ndrp1	—	—	$1.90 \times 10^{-3}$	-4.220	$2.46 \times 10^{-2}$	5.770
Nlk	—	—	$8.83 \times 10^{-6}$	-6.351	$5.06 \times 10^{-3}$	3.764
Npm1	—	—	$2.31 \times 10^{-3}$	-4.127	$9.32 \times 10^{-3}$	1.961
Pcna	$5.23 \times 10^{-3}$	3.688	$1.05 \times 10^{-3}$	-4.512	$7.92 \times 10^{-3}$	1.868
Prdx3	—	—	$4.70 \times 10^{-3}$	-3.781	$3.16 \times 10^{-3}$	2.099
Prom1	$1.87 \times 10^{-3}$	4.223	—	—	$4.27 \times 10^{-4}$	24.364
Ptp4a3	$9.89 \times 10^{-3}$	3.401	$2.58 \times 10^{-3}$	-4.067	$3.00 \times 10^{-2}$	2.064
Rara	$6.70 \times 10^{-3}$	3.578	$6.81 \times 10^{-3}$	-3.613	$8.85 \times 10^{-3}$	1.659
Rnd3	$2.80 \times 10^{-3}$	4.020	—	—	$2.55 \times 10^{-3}$	2.428
Slc7a5	$6.81 \times 10^{-3}$	3.573	—	—	$2.20 \times 10^{-3}$	9.769
Socs3	—	—	$7.94 \times 10^{-5}$	-5.403	$4.21 \times 10^{-3}$	8.617
Sult2a1	—	—	$2.56 \times 10^{-3}$	-4.069	$1.44 \times 10^{-2}$	7.438
Tgfa	—	—	$8.83 \times 10^{-6}$	-6.089	$1.08 \times 10^{-2}$	1.848
Xpa	—	—	$8.83 \times 10^{-6}$	-6.336	$7.80 \times 10^{-3}$	1.227

[Hyper-5mC & downregulated]				
Gene symbol	Hyper-5mC		Downregulated	
	<i>p</i> -Value	MAT-score <sup>a</sup>	<i>p</i> -Value	Fold-change
Apoa1	$3.91 \times 10^{-3}$	3.404	$2.36 \times 10^{-3}$	-1.483
Asph	$6.44 \times 10^{-4}$	4.062	$2.18 \times 10^{-2}$	-1.532
Cp	$9.96 \times 10^{-3}$	3.004	$6.15 \times 10^{-3}$	-1.207
Cxcl12	$2.73 \times 10^{-3}$	3.534	$3.31 \times 10^{-2}$	-2.813
Egfr	$2.65 \times 10^{-4}$	4.492	$3.18 \times 10^{-2}$	-3.202
Lepr	$8.26 \times 10^{-3}$	3.086	$1.73 \times 10^{-2}$	-1.354
Sox1	$4.21 \times 10^{-3}$	3.380	$2.14 \times 10^{-2}$	-1.672
Sox9	$9.50 \times 10^{-3}$	3.028	$1.19 \times 10^{-2}$	-6.940

<sup>a</sup> The relative methylation level calculated by the MAT (Model based Analysis of Tiling-arrays) algorithm. —: no change.



**Fig. 4** Gene networks built using the MetaCore database and our gene data. These genes were reported having interactions with (A) CAR and its downstream hub genes, (B) HNF4-alpha, (C) ESR1 and (D) HIF1A. These genes were also reported having relationships to tumors. Genes with red or blue circles indicate up-regulated or down-regulated genes compared to control, respectively. Green, red or gray arrows indicate positive/activation, negative/inhibition or unspecified effects, respectively.

**Table 4** Top 20 enrichment for hyper- and hypomethylated gene promoters by MetaCore pathways

Maps	Total	<i>p</i> -Value	FDR <sup>a</sup>	In data
Cytoskeleton remodeling_TGF, WNT and cytoskeletal remodeling	111	$4.81 \times 10^{-10}$	$2.21 \times 10^{-7}$	50
NF-AT signaling in cardiac hypertrophy	65	$5.06 \times 10^{-10}$	$2.21 \times 10^{-7}$	35
Neurophysiological process_dynenin–dynactin motor complex in axonal transport in neurons	54	$3.27 \times 10^{-9}$	$9.49 \times 10^{-7}$	30
Immune response_ oncostatin M signaling <i>via</i> MAPK in human cells	37	$7.95 \times 10^{-8}$	$1.43 \times 10^{-5}$	22
Development_cytokine-mediated regulation of megakaryopoiesis	57	$8.21 \times 10^{-8}$	$1.43 \times 10^{-5}$	29
Cell cycle_regulation of G1/S transition (part 1)	38	$1.55 \times 10^{-7}$	$2.25 \times 10^{-5}$	22
Cell adhesion_PLAU signaling	39	$2.90 \times 10^{-7}$	$3.61 \times 10^{-5}$	22
Development_epigenetic and transcriptional regulation of oligodendrocyte precursor cell differentiation and myelination	34	$4.00 \times 10^{-7}$	$4.36 \times 10^{-5}$	20
Immune response_ oncostatin M signaling <i>via</i> MAPK in mouse cells	35	$7.64 \times 10^{-7}$	$7.40 \times 10^{-5}$	20
Development_BMP signaling	33	$1.24 \times 10^{-6}$	$1.08 \times 10^{-4}$	19
Translation_regulation of EIF2 activity	39	$1.53 \times 10^{-6}$	$1.16 \times 10^{-4}$	21
Development_growth hormone signaling <i>via</i> PI3K/AKT and MAPK cascades	42	$1.60 \times 10^{-6}$	$1.16 \times 10^{-4}$	22
Ovarian cancer (main signaling cascades)	64	$1.84 \times 10^{-6}$	$1.24 \times 10^{-4}$	29
Cytoskeleton remodeling_cytoskeleton remodeling	102	$2.26 \times 10^{-6}$	$1.41 \times 10^{-4}$	40
Transcription_role of heterochromatin protein 1 (HP1) family in transcriptional silencing	40	$2.64 \times 10^{-6}$	$1.53 \times 10^{-4}$	21
Immune response_gastrin in inflammatory response	69	$3.54 \times 10^{-6}$	$1.93 \times 10^{-4}$	30
Immune response_HMGB1/RAGE signaling pathway	53	$3.85 \times 10^{-6}$	$1.97 \times 10^{-4}$	25
Development_TGF-beta-dependent induction of EMT <i>via</i> SMADs	35	$4.12 \times 10^{-6}$	$2.00 \times 10^{-4}$	19
Development_VEGF signaling <i>via</i> VEGFR2 – generic cascades	84	$5.66 \times 10^{-6}$	$2.50 \times 10^{-4}$	34
Development_role of HDAC and calcium/calmodulin-dependent kinase (CaMK) in control of skeletal myogenesis	54	$5.86 \times 10^{-6}$	$2.50 \times 10^{-4}$	25

<sup>a</sup> Multiple testing correction based on FDR (False Discovery Rate). Total number of enriched pathways for genes that were significantly changed ( $p < 0.01$ ) in 5mC by PB administration was 288.

**Table 5** Top 20 enrichment for hyper- and hypohydroxymethylated gene promoters by MetaCore pathways

Maps	Total	<i>p</i> -Value	FDR <sup>a</sup>	In data
Cytoskeleton remodeling_TGF, WNT and cytoskeletal remodeling	111	$2.63 \times 10^{-13}$	$2.31 \times 10^{-10}$	69
Signal transduction_AKT signaling	43	$1.06 \times 10^{-10}$	$4.65 \times 10^{-8}$	33
Development_PIP3 signaling in cardiac myocytes	47	$8.36 \times 10^{-10}$	$2.45 \times 10^{-7}$	34
Development_regulation of epithelial-to-mesenchymal transition (EMT)	64	$5.16 \times 10^{-9}$	$1.14 \times 10^{-6}$	41
NF-AT signaling in cardiac hypertrophy	65	$1.01 \times 10^{-8}$	$1.49 \times 10^{-6}$	41
Development_IGF-1 receptor signaling	52	$1.01 \times 10^{-8}$	$1.49 \times 10^{-6}$	35
Immune response_IL-1 signaling pathway	44	$1.33 \times 10^{-8}$	$1.67 \times 10^{-6}$	31
Some pathways of EMT in cancer cells	51	$2.39 \times 10^{-8}$	$2.63 \times 10^{-6}$	34
Main growth factor signaling cascades in multiple myeloma cells	41	$3.42 \times 10^{-8}$	$3.34 \times 10^{-6}$	29
Colorectal cancer (general schema)	30	$8.08 \times 10^{-8}$	$6.34 \times 10^{-6}$	23
Immune response_signaling pathway mediated by IL-6 and IL-1	30	$8.08 \times 10^{-8}$	$6.34 \times 10^{-6}$	23
Development_epigenetic and transcriptional regulation of oligodendrocyte precursor cell differentiation and myelination	34	$8.96 \times 10^{-8}$	$6.34 \times 10^{-6}$	25
Signal transduction_additional pathways of NF-kB activation (in the cytoplasm)	53	$1.01 \times 10^{-7}$	$6.34 \times 10^{-6}$	34
Development_insulin, IGF-1 and TNF-alpha in brown adipocyte differentiation	53	$1.01 \times 10^{-7}$	$6.34 \times 10^{-6}$	34
Immune response_gastrin in inflammatory response	69	$1.16 \times 10^{-7}$	$6.71 \times 10^{-6}$	41
IGF family signaling in colorectal cancer	60	$1.25 \times 10^{-7}$	$6.71 \times 10^{-6}$	37
Transcription_N-CoR/SMRT complex-mediated epigenetic gene silencing	49	$1.30 \times 10^{-7}$	$6.71 \times 10^{-6}$	32
Development_regulation of lung epithelial progenitor cell differentiation	41	$1.93 \times 10^{-7}$	$9.45 \times 10^{-6}$	28
Cell adhesion_PLAU signaling	39	$2.08 \times 10^{-7}$	$9.61 \times 10^{-6}$	27
Development_TGF-beta-dependent induction of EMT <i>via</i> SMADs	35	$2.27 \times 10^{-7}$	$1.00 \times 10^{-5}$	25

<sup>a</sup> Multiple testing correction based on FDR (False Discovery Rate). Total number of enriched pathways for genes that were significantly changed ( $p < 0.01$ ) in 5hmC by PB administration was 366.

would like to know gene contributors with epigenetic alterations to PB-induced liver tumorigenesis, we focused on up and down regulated genes with changes in 5mC/5hmC in this paper. These tumors have distinctive alterations of 5mC and 5hmC profiles in thousands of gene promoter regions, suggesting that DNA modifications may characterize liver

tumors in PB-treated mice as well as hepatic cancers in humans.<sup>16,17</sup> In comparison with the number of differential gene promoters, there are more 5hmC-altered promoters than 5mC. This difference may be partially due to a structural difference between hydroxymethyl and methyl groups. The former group is slightly larger than the latter, which results in a

**Table 6** Top 20 enrichment for expression-changed genes by MetaCore pathways

Maps	Total	p-Value	FDR <sup>a</sup>	In data
Cytoskeleton remodeling_TGF, WNT and cytoskeletal remodeling	111	$3.04 \times 10^{-11}$	$2.73 \times 10^{-8}$	47
Immune response_IL-4-induced regulators of cell growth, survival, differentiation and metabolism	63	$1.48 \times 10^{-10}$	$6.63 \times 10^{-8}$	32
Cell cycle_ESR1 regulation of G1/S transition	33	$7.70 \times 10^{-9}$	$1.99 \times 10^{-6}$	20
Blood coagulation_blood coagulation	39	$8.88 \times 10^{-9}$	$1.99 \times 10^{-6}$	22
Immune response_IL-6 signaling pathway via JAK/STAT	72	$4.39 \times 10^{-8}$	$7.89 \times 10^{-6}$	31
Cell cycle_the metaphase checkpoint	36	$6.03 \times 10^{-8}$	$9.02 \times 10^{-6}$	20
IGF family signaling in colorectal cancer	60	$1.07 \times 10^{-7}$	$1.25 \times 10^{-5}$	27
Immune response_oncostatin M signaling via MAPK in human cells	37	$1.12 \times 10^{-7}$	$1.25 \times 10^{-5}$	20
Cytoskeleton remodeling_cytoskeleton remodeling	102	$1.48 \times 10^{-7}$	$1.47 \times 10^{-5}$	38
Oxidative phosphorylation	105	$3.52 \times 10^{-7}$	$3.07 \times 10^{-5}$	38
Protein folding and maturation_POMC processing	30	$4.10 \times 10^{-7}$	$3.07 \times 10^{-5}$	17
Regulation of lipid metabolism_RXR-dependent regulation of lipid metabolism via PPAR, RAR and VDR	30	$4.10 \times 10^{-7}$	$3.07 \times 10^{-5}$	17
Development_WNT signaling pathway. Part 2	53	$4.72 \times 10^{-7}$	$3.26 \times 10^{-5}$	24
Neurophysiological process_dynein-dynactin motor complex in axonal transport in neurons	54	$7.21 \times 10^{-7}$	$4.63 \times 10^{-5}$	24
Cell adhesion_chemokines and adhesion	100	$8.26 \times 10^{-7}$	$4.95 \times 10^{-5}$	36
Immune response_oncostatin M signaling via MAPK in mouse cells	35	$1.28 \times 10^{-6}$	$7.20 \times 10^{-5}$	18
Cell cycle_role of APC in cell cycle regulation	32	$1.40 \times 10^{-6}$	$7.41 \times 10^{-5}$	17
Immune response_alternative complementary pathway	53	$2.04 \times 10^{-6}$	$1.02 \times 10^{-4}$	23
Cell cycle_chromosome condensation in prometaphase	21	$2.50 \times 10^{-6}$	$1.18 \times 10^{-4}$	13
Cytoskeleton remodeling_role of PKA in cytoskeleton reorganisation	40	$3.06 \times 10^{-6}$	$1.37 \times 10^{-4}$	19

<sup>a</sup> Multiple testing correction based on FDR (False Discovery Rate). Total number of enriched pathways for genes that were significantly changed ( $p < 0.01$ ) in gene expression by PB administration was 231.

higher titer of 5hmC antibodies and more sensitive detection of 5hmC sites than 5mC. In addition, the correlation between 5hmC alterations and up-regulated genes induced by PB treatment is clearer and more significant than 5mC alterations in mice.<sup>9,23</sup>

We performed integrated analysis and found that hundreds of genes are coordinately altered in DNA modification and expression in the liver of PB-treated mice. Subsequently, gene network analysis showed that several genes showing relationship between the CAR and tumor development are reported. Phillips *et al.* reported genes which showed CAR-dependent increases or decreases in liver tumors of mice,<sup>19</sup> so we compared our data with their data. We found that some epigenetically and transcriptionally changed genes are reported to be transcriptionally changed in PB-treated wild-type mice but not changed in PB-treated CAR-knockout mice. For example, CAR activation results in direct up-regulation of Mdm2 expression,<sup>8</sup> which is purportedly involved in poor survival in patients with hepatocellular carcinoma (HCC).<sup>58</sup> Anxa2, whose promoter might contain CAR response elements,<sup>19</sup> is expressed more abundantly in HCC tissues than in non-tumorous tissues.<sup>59</sup> The CAR opposes the action of the estrogen receptor (Esr1),<sup>60</sup> and Esr1 regulates the cell cycle by up-regulating Mki67.<sup>61</sup> Some reports show that the high Mki67 expression may be correlated with the cell proliferation of HCC.<sup>38,62,63</sup> The CAR probably binds to the PB-responsive enhancer module of the hypoxia inducible factor (HIF)-1A,<sup>64</sup> which may contribute to HIF1A-induced activation of Cyr61.<sup>65</sup> Cyr61 may relate to invasion and metastasis of HCC.<sup>66</sup> These genes illustrated above might play a crucial function in PB-induced liver tumorigenesis in mice.

Another previous publication has reported candidate biomarkers of PB exposure up to 13 weeks of exposure that are differentially expressed correlated with epigenetic changes.<sup>23</sup> We also compared our data with those of Laird *et al.* (2013)<sup>9</sup> and Thomson *et al.* (2013)<sup>23</sup> and found that 2 genes (Ndr1 and Prom1) exhibit the changes in 5hmC levels with induced gene expression in both. Under short-term hypoxia, Ndr1 expression is induced in a HIF1A-dependent manner.<sup>67</sup> Ndr1 is known to be associated with metastasis, recurrence and poor prognosis in HCC.<sup>68</sup> HIF1A increases the promoter activity of Prom1,<sup>69</sup> whose expression may indicate high capacity for tumorigenicity in HCC cells.<sup>70</sup> These two genes showed continuous change in both 5hmC and gene expression levels from short-term PB-treated liver to long-term PB-induced tumor, suggesting that these genes might also be responsible for a cancer-promoting effect by PB.

Pathway enrichment analysis discovered many pathways enriched significantly, which included our data in about half of the total genes. Interestingly, the major types of top 20 pathways enriched for 5mC- or 5hmC-altered genes show different trends from those for transcriptionally altered genes. Many pathways enriched for gene expression profiles are associated with the cell cycle. This result supports the previous studies that PB administration to B6C3F1 mice or wild-type C57BL/6 mice causes increased expression of cell cycle regulatory genes.<sup>20,45</sup> In contrast, both enrichment results for 5mC and 5hmC profiles contain fewer pathways related to cell cycle regulation and more pathways related to development and cancer than gene expression. These differences suggest that the activation of signaling pathways leading to tumorigenesis is more characteristically associated with DNA modification than gene expression.

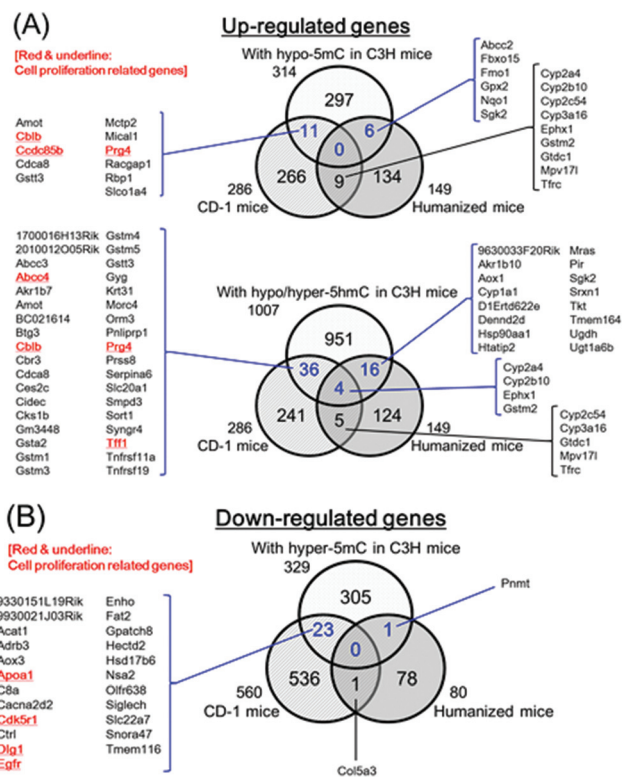


**Fig. 5** Overlap between the genes with 5mC and 5hmC alterations in mouse hepatocellular adenoma induced by DEN/PB and altered genes of liver in CD-1 and humanized chimeric mice treated with PB for 7 days. (A) and (B) present up-regulated or down-regulated genes compared to control, respectively. “C3H mice” means hepatocellular adenoma induced by DEN/PB. The altered genes of non-tumor liver in CD-1 and humanized chimeric mice treated with PB for 7 days were previously published.<sup>39</sup> Information of individual genes overlapping is presented in ESI Tables S5–7.†

A recent controversy concerning the CAR-mediated MOA for mouse liver tumor formation concerns the phenotype of mouse liver tumors promoted by PB, where beta-catenin gene mutations have been observed.<sup>48,49</sup> This gene is often mutated in human liver tumors.<sup>71</sup> In our data, the promoter region of the beta-catenin gene was hypermethylated (chr9: 120778584–120779193) and hypohydroxymethylated (chr9: 120780888–120781871), but beta-catenin gene expression was not significantly altered based on the criteria of our study (but close to significant,  $p = 0.0543$ , 1.22-fold control). Furthermore, we performed additional gene network analysis of the Wnt/beta-catenin signaling network in MetaCore with our gene expression data of the three animal models (Fig. 6). PB treatment altered the expression of many genes related to the Wnt/beta-catenin signaling network in tumor tissue of C3H mice (51 genes) and in the liver of CD-1 mice (36 genes), however, fewer in chimeric mice with human hepatocytes (12 genes). These findings suggest a species difference between the effects of PB in mouse and human hepatocytes.

As shown in Fig. 5 and Table 6, we identified nine genes altered in common in hepatocellular adenoma induced by

DEN/PB (both alterations of expression and 5mC/5hmC) and in the liver of mice treated with PB for 1 week (alteration of expression, 5mC/5hmC were not determined). Interestingly, all nine genes were known as cell proliferation/growth-related genes, and seven of the nine genes were also known to relate to CAR or beta-catenin. Thus, taking published information into consideration, the determined nine genes, at least, could provide important information for an evaluation of key genes for CAR-mediated mouse liver tumorigenesis.

The present research may have limitations for reaching the definitive conclusions described above. Dose levels were different between the 27 week and 1 week studies; much higher doses were used in the short duration studies (500 ppm for a 27 week study and 2500 ppm for 1 week). This lack of dose concordance may render conclusions based on similarity between short and long duration as speculative and may not provide strong evidence for inclusion into the mouse MOA for liver tumorigenesis. However, in the 1 week study in CD-1 mice, NaPB equivocally increased hepatic 7-pentoxoresorufin *O*-depentylase activity (CYP2B marker) at 500, 1000, 1500 and 2500 ppm (4.4, 5.4, 6.4 and 6.4 fold of control).<sup>39</sup> These data suggest that CAR activation by PB 500 and 2500 ppm was similar. Thus, we consider that the similarity between short and long duration can provide evidence for inclusion into the mouse MOA. To confirm this, functional analysis of the selected genes remains to be conducted. Another limitation was the confounded study design. We analyzed the tumor/PB vs. non-tumor/control liver from different animals, but this analysis cannot separate PB-specific effects from tumor-specific effects. This means that the identified changed genes carried over into the subsequent analysis may be a result of either the PB treatment or the tumorigenesis process or the interaction of the two. Therefore, when compared with the short duration treatments, any commonality may be due merely to a PB response that is sustained for the duration of treatment. Thus, functional analysis of the selected genes remains to be evaluated in tumorigenesis.

#### Evaluation of the human relevance of the CAR-mediated MOA for mouse hepatocellular tumorigenesis

In the present study, plasma PB levels in the DEN/500 ppm PB mice were  $15 \mu\text{g ml}^{-1}$ . The plasma levels of PB observed in human subjects given therapeutic doses of 3–6 mg  $\text{kg}^{-1}$  ranged from 10 to  $25 \mu\text{g ml}^{-1}$ .<sup>72</sup> Therefore, plasma PB levels in the DEN/500 ppm PB mice were equivalent to those reported in humans by Monro (1993).<sup>72</sup> Since plasma PB levels in the humanized chimeric mice treated with 1000 ppm ( $75 \mu\text{g ml}^{-1}$ ) were higher than those in the DEN/500 ppm PB mice ( $15 \mu\text{g ml}^{-1}$ ) but equivalent to those in CD-1 mice treated with 2500 ppm ( $70 \mu\text{g ml}^{-1}$ ), we believe that the comparison between the 1000 ppm PB treated humanized chimeric mice and the DEN/500 ppm PB treated mice, and the 2500 ppm PB treated mice is able to provide useful information, at least without underestimation, on species differences in initial key events of hepatocellular tumorigenesis. Non-overlap of the selected nine cell proliferation/growth-related genes described

**Table 7** Overlapping genes between hepatocellular adenoma induced by DEN/500 ppm PB in C3H mice and livers in CD-1 mice treated with 2500 ppm PB for 7 days: detailed information of genes with gene ontology terms of relationship to CAR or beta-catenin and/or cell proliferation based on published references

Gene symbol (mouse)	C3H mice (up-regulated)		Gene ontology terms of relationship to:		Ref.
	<i>p</i> -Value	Fold-change	CAR or beta-catenin	Cell proliferation or cell growth	
Abcc4	$8.93 \times 10^{-5}$	104.2	Activation of CAR induces hepatic up-regulation of Abcc4 in a CAR-dependent manner.	Abcc4 enhances cell growth by progressing cell cycle.	73 74
Cblb	$4.21 \times 10^{-2}$	2.2	—	Cblb regulates growth factor receptor signaling negatively and is involved in the inhibition of cancer cell proliferation. Ccdc85b inhibits tumor cell growth.	75
Ccdc85b	$7.77 \times 10^{-3}$	1.6	Ccdc85b activates the degradation of beta-catenin.	—	76
Prg4	$1.09 \times 10^{-2}$	1.8	Activation of Wnt/beta-catenin signaling increases Prg4 expression and slow-cell cycle population.	Prg4 suppresses synovial cell proliferation.	77
Tff1	$1.97 \times 10^{-4}$	16.3	Tff1 promotes invasion and chemoresistance in cancer through Wnt/beta-catenin signaling.	Tff1 reduces cell proliferation by delaying G1-S cell cycle transition.	78 79 80
Gene ontology terms of relationship to:					
Gene symbol (mouse)	C3H mice (down-regulated)		Cell proliferation or cell growth		Ref.
	<i>p</i> -Value	Fold-change	CAR or beta-catenin	Cell proliferation or cell growth	
Apoa1	$2.36 \times 10^{-3}$	-1.5	Activation of CAR decreases plasma HDL level through down-regulation of Apoa1 expression.	Apoa1 promotes proliferation of human endothelial progenitor cells.	81
Cdk5r1	$2.43 \times 10^{-2}$	-1.2	—	Cdk5r1 has a role of induction in beta-cell proliferation.	82
Dlg1	$9.79 \times 10^{-3}$	-1.6	Beta-catenin contributes to tumorigenesis through inducing DLG degradation (anti-Dlg1 antibody was used in this study).	Dlg1 is involved in inhibition of cell cycle progression by blocking G0/G1 transition.	83 84
Egfr	$3.18 \times 10^{-2}$	-3.2	Phenobarbital activates CAR by repressing the Egfr signaling.	Egfr signaling play key roles in hepatic cell proliferation.	85 86 87

—: not found in the published literature.

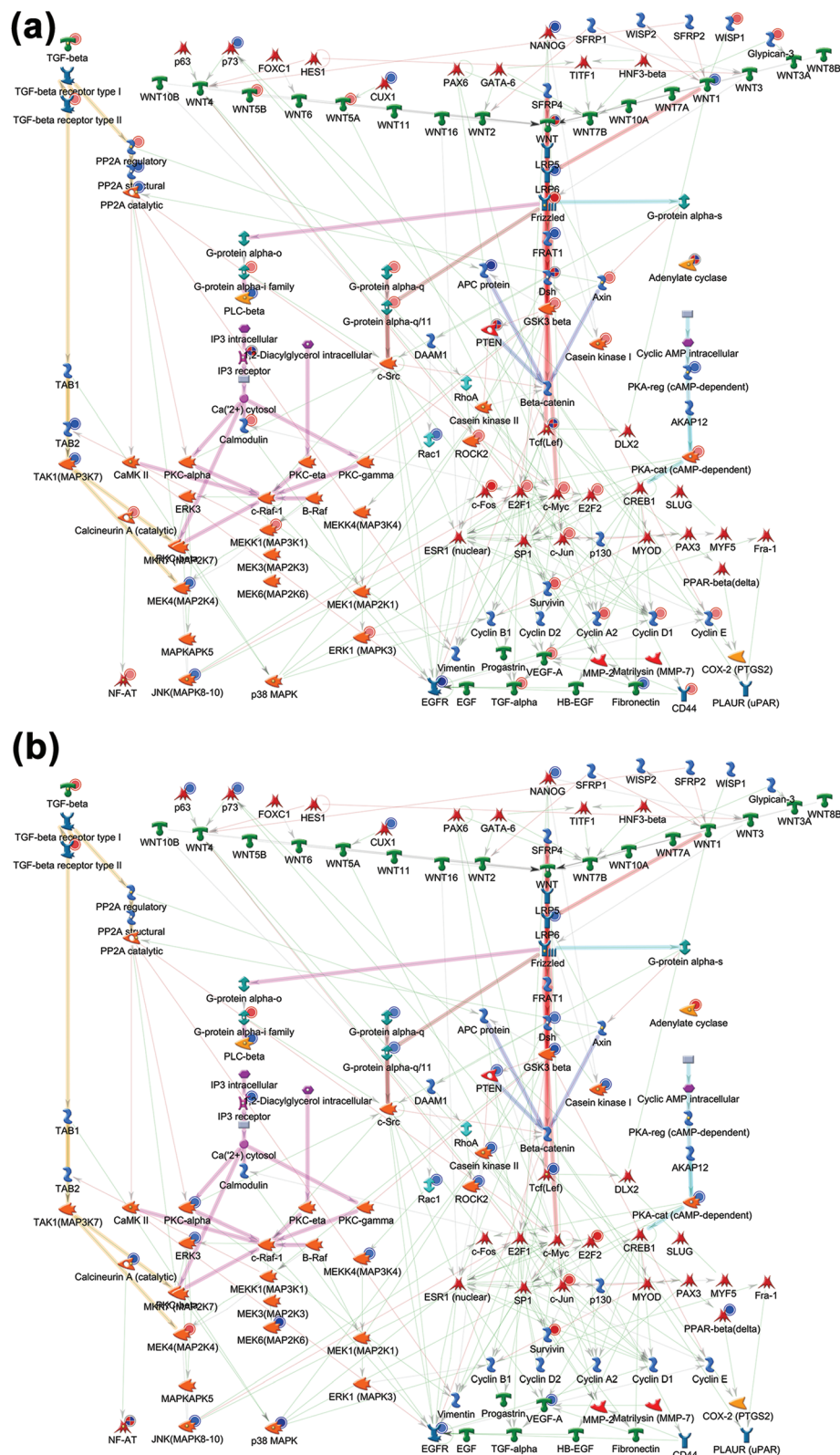


**Fig. 6** Gene network of Wnt signaling in the MetaCore database and the gene expression data of (A) hepatocellular adenoma in C3H mice, (B) liver in CD-1 mice and (C) chimeric mice with human hepatocytes. Genes with red or blue circles indicate up-regulated or down-regulated genes compared to control, respectively. Green, red or gray arrows indicate positive/activation, negative/inhibition or unspecified effects, respectively.

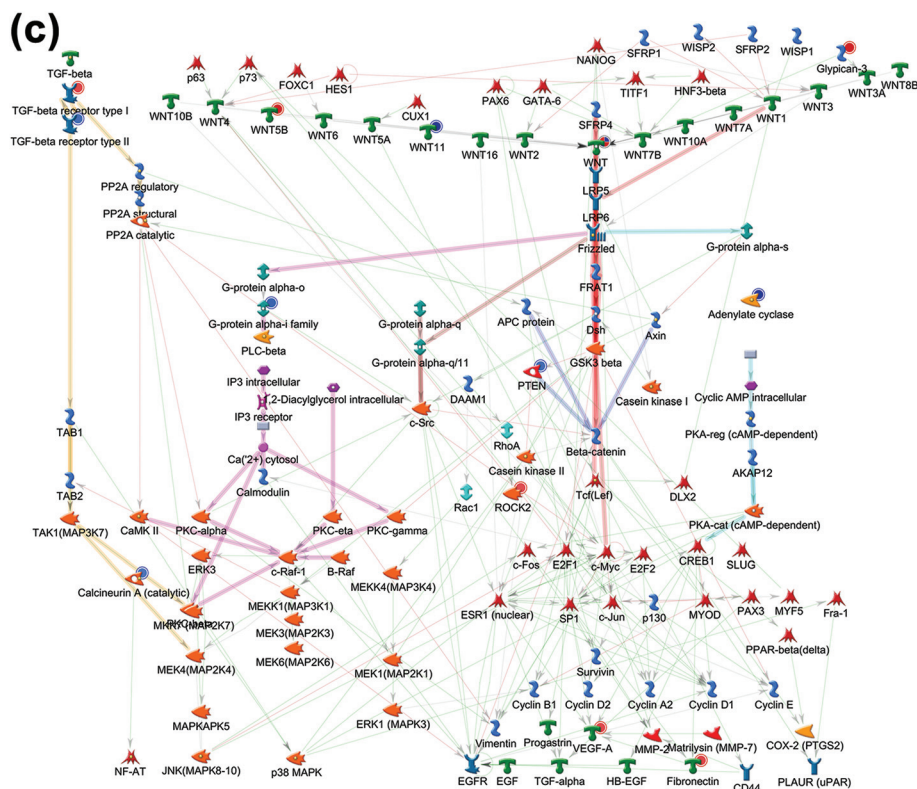


Fig. 6 (Contd).

above in humanized chimeric mouse models (namely, nine cell proliferation/growth-related genes observed in the liver of mice given PB for 1 week and in DEN/PB liver tumors of mice given PB for 27 weeks were not increased in the humanized chimeric mice given PB for 1 week) does not conflict with the previous findings that the key species differences are related to the lack of cell proliferation in human hepatocytes.<sup>31,39,41,43</sup> Therefore, these findings are consistent with the previous conclusion that CAR-mediated MOA for rodent liver tumorigenesis is not relevant to humans.<sup>3,27–42</sup> To confirm this, functional analysis of the selected genes remains to be evaluated in mouse liver tumorigenesis.

## Funding

This work was supported by the Sumitomo Chemical Company, Ltd.

## Conflicts of interest

There are no conflicts to declare.

## Acknowledgements

We acknowledge Professor Samuel M. Cohen (Department of Pathology and Microbiology, University of Nebraska Medical

Center) and Professor Brian G. Lake (Centre for Toxicology, Faculty of Health and Medical Sciences, University of Surrey) for valuable scientific advice. The authors also thank Mr N. Hattori for global DNA methylation, hydroxymethylation and gene expression analyses; Ms N. Takata for preliminary experiments of MeDIP; and Ms H. Kikumoto and K. Tanaka for experimental animal studies in this work.

## References

- 1 IARC, *IARC Monographs on the Evaluation of Carcinogenic Risks to Humans. Some Thyrotropic Agents: Phenobarbital and its sodium salt*, 2001, vol. 79, pp. 161–288.
- 2 T. Kawamoto, T. Sueyoshi, I. Zelko, R. Moore, K. Washburn and M. Negishi, Phenobarbital-responsive nuclear translocation of the receptor CAR in induction of the CYP2B gene, *Mol. Cell. Biol.*, 1999, **19**, 6318–6322.
- 3 C. R. Elcombe, R. C. Peffer, D. C. Wolf, J. Bailey, R. Bars, D. Bell, R. C. Cattley, S. S. Ferguson, D. Geter, A. Goetz, J. I. Goodman, S. Hester, A. Jacobs, C. J. Omiecinski, R. Schoeny, W. Xie and B. G. Lake, Mode of action and human relevance analysis for nuclear-receptor mediated liver toxicity: a case study with phenobarbital as a model constitutive androstane receptor (CAR) activator, *Crit. Rev. Toxicol.*, 2014, **44**, 64–82.
- 4 P. Honkakoski, I. Zelko, T. Sueyoshi and M. Negishi, The nuclear orphan receptor CAR-retinoid X receptor hetero-

- dimer activates the phenobarbital-responsive enhancer module of the CYP2B gene, *Mol. Cell. Biol.*, 1998, **18**, 5652–5658.
- 5 K. Kobayashi, T. Sueyoshi, K. Inoue, R. Moore and M. Negishi, Cytoplasmic accumulation of the nuclear receptor CAR by a tetratricopeptide repeat protein in HepG2 cells, *Mol. Pharmacol.*, 2003, **64**, 1069–1075.
  - 6 K. Yoshinari, K. Kobayashi, R. Moore, T. Kawamoto and M. Negishi, Identification of the nuclear receptor CAR: HSP90 complex in mouse liver and recruitment of protein phosphatase 2A in response to phenobarbital, *FEBS Lett.*, 2003, **548**, 17–20.
  - 7 Y. Yamamoto, R. Moore, T. L. Goldsworthy, M. Negishi and R. R. Maronpot, The orphan nuclear receptor constitutive active/androstane receptor is essential for liver tumor promotion by phenobarbital in mice, *Cancer Res.*, 2004, **64**, 7197–7200.
  - 8 W. Huang, J. Zhang, M. Washington, J. Liu, J. M. Parant, G. Lozano and D. D. Moore, Xenobiotic Stress Induces Hepatomegaly and Liver Tumors via the Nuclear Receptor Constitutive Androstane Receptor, *Mol. Endocrinol.*, 2005, **19**, 1646–1653.
  - 9 A. Laird, J. P. Thomson, D. J. Harrison and R. R. Meehan, 5-Hydroxymethylcytosine profiling as an indicator of cellular state, *Epigenomics*, 2013, **5**, 655–669.
  - 10 L. D. Moore, T. Le and G. Fan, DNA methylation and its basic function, *Neuropsychopharmacology*, 2013, **38**, 23–38.
  - 11 C. J. Mariani, J. Madzo, E. L. Moen, A. Yesilkalan and L. A. Godley, Alterations of 5-hydroxymethylcytosine in human cancers, *Cancers*, 2013, **5**, 786–814.
  - 12 J. P. Reddington, S. Pennings and R. R. Meehan, Non-canonical functions of the DNA methylome in gene regulation, *Biochem. J.*, 2013, **451**, 13–23.
  - 13 E. L. Moen, C. J. Mariani, H. Zullo, M. Jeff-Eke, E. Litwin, J. N. Nikitas and L. A. Godley, New themes in the biological functions of 5-methylcytosine and 5-hydroxymethylcytosine, *Immunol. Rev.*, 2015, **253**, 36–49.
  - 14 H. Kaneto, S. Sasaki, H. Yamamoto, F. Itoh, M. Toyota, H. Suzuki, I. Ozeki, N. Iwata, T. Ohmura, T. Satoh, Y. Karino, J. Toyota, M. Satoh, T. Endo, M. Omata and K. Imai, Detection of hypermethylation of the p16(INK4A) gene promoter in chronic hepatitis and cirrhosis associated with hepatitis B or C virus, *Gut*, 2001, **48**, 372–377.
  - 15 E. L. Sceusi, D. S. Loose and C. J. Wray, Clinical implications of DNA methylation in hepatocellular carcinoma, *HPB*, 2011, **13**, 369–376.
  - 16 W.-R. Liu, M.-X. Tian, L. Jin, L.-X. Yang, Z.-B. Ding, Y.-H. Shen, Y.-F. Peng, J. Zhou, S.-J. Qiu, Z. Dai, J. Fan and Y.-H. Shi, High expression of 5-hydroxymethylcytosine and isocitrate dehydrogenase 2 is associated with favorable prognosis after curative resection of hepatocellular carcinoma, *J. Exp. Clin. Cancer Res.*, 2014, **33**, 32.
  - 17 S. O. Sajadian, S. Ehnert, H. Vakilian, E. Koutsouraki, G. Damm, D. Seehofer, W. Thasler, S. Dooley, H. Baharvand, B. Sipos and A. K. Nussler, Induction of active demethylation and 5hmC formation by 5-azacytidine is TET2 dependent and suggests new treatment strategies against hepatocellular carcinoma, *Clin. Epigenet.*, 2015, **7**, 98.
  - 18 J. P. Thomson and R. R. Meehan, The application of genome-wide 5-hydroxymethylcytosine studies in cancer research, *Epigenomics*, 2016, **9**, 77–91.
  - 19 J. M. Phillips, L. D. Burgoon and J. I. Goodman, The constitutive active/androstane receptor facilitates unique phenobarbital-induced expression changes of genes involved in key pathways in precancerous liver and liver tumors, *Toxicol. Sci.*, 2009, **110**, 319–333.
  - 20 J. M. Phillips, L. D. Burgoon and J. I. Goodman, Phenobarbital elicits unique, early changes in the expression of hepatic genes that affect critical pathways in tumor-prone B6C3F1 mice, *Toxicol. Sci.*, 2009, **109**, 193–205.
  - 21 H. Lempiäinen, A. Muller, S. Brasa, S. S. Teo, T. C. Roloff, L. Morawiec, N. Zamurovic, A. Vicart, E. Funhoff, P. Couttet, D. Schubeler, O. Grenet, J. Marlowe, J. Moggs and R. Terranova, Phenobarbital mediates an epigenetic switch at the constitutive androstane receptor (CAR) target gene *Cyp2b10* in the liver of B6C3F1 mice, *PLoS One*, 2011, **6**, e18216.
  - 22 J. P. Thomson, H. Lempiäinen, J. A. Hackett, C. E. Nestor, A. Muller, F. Bolognani, E. J. Oakeley, D. Schubeler, R. Terranova, D. Reinhardt, J. G. Moggs and R. R. Meehan, Non-genotoxic carcinogen exposure induces defined changes in the 5-hydroxymethylome, *Genome Biol.*, 2012, **13**, R93.
  - 23 J. P. Thomson, J. M. Hunter, H. Lempiäinen, A. Muller, R. Terranova, J. G. Moggs and R. R. Meehan, Dynamic changes in 5-hydroxymethylation signatures underpin early and late events in drug exposed liver, *Nucleic Acids Res.*, 2013, **41**, 5639–5654.
  - 24 A. N. Bachman, J. M. Phillips and J. I. Goodman, Phenobarbital induces progressive patterns of GC-rich and gene-specific altered DNA methylation in the liver of tumor-prone B6C3F1 mice, *Toxicol. Sci.*, 2006, **91**, 393–405.
  - 25 J. M. Phillips and J. I. Goodman, Multiple genes exhibit phenobarbital-induced constitutive active/androstane receptor-mediated DNA methylation changes during liver tumorigenesis and in liver tumors, *Toxicol. Sci.*, 2009, **108**, 273–289.
  - 26 J. P. Thomson, R. Ottaviano, E. B. Unterberger, H. Lempiäinen, A. Muller, R. Terranova, R. S. Illingworth, S. Webb, A. R. W. Kerr, M. J. Lyall, A. J. Drake, C. R. Wolf, J. G. Moggs, M. Schwarz and R. R. Meehan, Loss of Tet1-associated 5-hydroxymethylcytosine is concomitant with aberrant promoter hypermethylation in liver cancer, *Cancer Res.*, 2016, **76**, 3097–3108.
  - 27 S. M. Cohen and L. L. Arnold, Chemical Carcinogenesis, *Toxicol. Sci.*, 2011, **120**, S76–S92.
  - 28 S. M. Cohen, Evaluation of possible carcinogenic risk to humans based on liver tumors in rodent assays: the two-year bioassay is no longer necessary, *Toxicol. Pathol.*, 2010, **38**, 487–501.
  - 29 M. P. Holsapple, H. C. Pitot, S. M. Cohen, A. R. Boobis, J. E. Klaunig, T. Pastoor, V. L. Dellarco and Y. P. Dragan,



- Mode of action in relevance of rodent liver tumors to human cancer risk, *Toxicol. Sci.*, 2006, **89**, 51–56.
- 30 B. G. Lake, Species differences in the hepatic effects of inducers of CYP2B and CYP4A subfamily forms: relationship to rodent liver tumour formation, *Xenobiotica*, 2009, **39**, 582–596.
- 31 Y. Hirose, H. Nagahori, T. Yamada, Y. Deguchi, Y. Tomigahara, K. Nishioka, S. Uwagawa, S. Kawamura, N. Isobe, B. G. Lake and Y. Okuno, Comparison of the effects of the synthetic pyrethroid Metofluthrin and phenobarbital on CYP2B form induction and replicative DNA synthesis in cultured rat and human hepatocytes, *Toxicology*, 2009, **258**, 64–69.
- 32 T. Yamada, S. Uwagawa, Y. Okuno, S. M. Cohen and H. Kaneko, Case study: an evaluation of the human relevance of the synthetic pyrethroid metofluthrin-induced liver tumors in rats based on mode of action, *Toxicol. Sci.*, 2009, **108**, 59–68.
- 33 T. G. Osimitz and B. G. Lake, Mode-of-action analysis for induction of rat liver tumors by pyrethrins: relevance to human cancer risk, *Crit. Rev. Toxicol.*, 2009, **39**, 501–511.
- 34 B. G. Lake, R. J. Price and T. G. Osimitz, Mode of action analysis for pesticide-induced rodent liver tumours involving activation of the constitutive androstane receptor: relevance to human cancer risk, *Pest Manage. Sci.*, 2015, **71**, 829–834.
- 35 M. J. LeBaron, B. B. Gollapudi, C. Terry, R. Billington and R. J. Rasoulpour, Human relevance framework for rodent liver tumors induced by the insecticide sulfoxaflor, *Crit. Rev. Toxicol.*, 2014, **44**(Suppl. 2), 15–24.
- 36 M. J. LeBaron, R. J. Rasoulpour, B. B. Gollapudi, R. Sura, H. L. Kan, M. R. Schisler, L. H. Pottenger, S. Papineni and D. L. Eisenbrandt, Characterization of nuclear receptor-mediated murine hepatocarcinogenesis of the herbicide pronamide and its human relevance, *Toxicol. Sci.*, 2014, **142**, 74–92.
- 37 P. Marx-Stoelting, K. Ganzenberg, C. Knebel, F. Schmidt, S. Rieke, H. Hammer, F. Schmidt, O. Potz, M. Schwarz and A. Braeuning, Hepatotoxic effects of cyproconazole and prochloraz in wild-type and hCAR/hPXR mice, *Arch. Toxicol.*, 2017, **91**, 2895–2907.
- 38 C. E. Wood, R. R. Hukkanen, R. Sura, D. Jacobson-Kram, T. Nolte, M. Odin and S. M. Cohen, Scientific and regulatory policy committee (SRPC) review: Interpretation and use of cell proliferation data in cancer risk assessment, *Toxicol. Pathol.*, 2015, **43**, 760–775.
- 39 T. Yamada, Y. Okuda, M. Kushida, K. Sumida, H. Takeuchi, H. Nagahori, T. Fukuda, B. G. Lake, S. M. Cohen and S. Kawamura, Human hepatocytes support the hypertrophic but not the hyperplastic response to the murine nongenotoxic hepatocarcinogen sodium phenobarbital in an *in vivo* study using a chimeric mouse with humanized liver, *Toxicol. Sci.*, 2014, **142**, 137–157.
- 40 T. Yamada, S. M. Cohen and B. G. Lake, The mode of action for phenobarbital-induced rodent liver tumor formation is not relevant for humans: Recent studies with humanized mice. Letters to the Editor, *Toxicol. Sci.*, 2015, **147**, 298–299.
- 41 T. Yamada, H. Kikumoto, B. G. Lake and S. Kawamura, Lack of effect of metofluthrin and sodium phenobarbital on replicative DNA synthesis and Ki-67 mRNA expression in cultured human hepatocytes, *Toxicol. Res.*, 2015, **4**, 901–913.
- 42 M. Kushida, T. Yamada and Y. Okuno, in *Thresholds of Genotoxic Carcinogens*, ed. T. Nomi and S. Fukushima, Academic Press, London, 2016, ch. 12, pp. 193–203.
- 43 W. Parzefall, E. Erber, R. Sedivy and R. Schulte-Hermann, Testing for induction of DNA synthesis in human hepatocyte primary cultures by rat liver tumor promoters, *Cancer Res.*, 1991, **51**, 1143–1147.
- 44 C. La Vecchia and E. Negri, A review of epidemiological data on epilepsy, phenobarbital, and risk of liver cancer, *Eur. J. Cancer Prev.*, 2014, **23**, 1–7.
- 45 R. Luisier, H. Lempiainen, N. Schlerbichler, A. Braeuning, M. Geissler, V. Dubost, A. Muller, N. Scheer, S. D. Chibout, H. Hara, F. Picard, D. Theil, P. Couttet, A. Vitobello, O. Grenet, B. Grasl-Kraupp, H. Ellinger-Ziegelbauer, J. P. Thomson, R. R. Meehan, C. R. Elcombe, C. J. Henderson, C. R. Wolf, M. Schwarz, P. Moulin, R. Terranova and J. G. Moggs, Phenobarbital induces cell cycle transcriptional responses in humanized CAR/PXR mouse liver, *Toxicol. Sci.*, 2014, **139**, 501–511.
- 46 A. Braeuning, A. Gavrilov, S. Brown, C. R. Wolf, C. J. Henderson and M. Schwarz, Phenobarbital-mediated tumor promotion in transgenic mice with humanized CAR and PXR, *Toxicol. Sci.*, 2014, **140**, 259–270.
- 47 A. Braeuning, Liver cell proliferation and tumor promotion by phenobarbital: relevance for humans?, *Arch. Toxicol.*, 2014, **88**, 1771–1772.
- 48 A. Braeuning and M. Schwarz, Is the question of phenobarbital as potential liver cancer risk factor for humans really resolved?, *Arch. Toxicol.*, 2016, **90**, 1525–1526.
- 49 A. Braeuning, C. J. Henderson, C. R. Wolf and M. Schwarz, Model systems for understanding mechanisms of nongenotoxic carcinogenesis; response, *Toxicol. Sci.*, 2015, **147**, 299–300.
- 50 N. Groll, F. Kollotzek, J. Goepfert, T. O. Joos, M. Schwarz and A. Braeuning, Phenobarbital inhibits calpain activity and expression in mouse hepatoma cells, *Biol. Chem.*, 2016, **397**, 91–96.
- 51 J. M. Phillips and J. I. Goodman, Identification of genes that may play critical roles in phenobarbital (PB)-induced liver tumorigenesis due to altered DNA methylation, *Toxicol. Sci.*, 2008, **104**, 86–99.
- 52 Y. Sakamoto, K. Inoue, M. Takahashi, Y. Taketa, Y. Kodama, K. Nemoto, M. Degawa, T. Gamou, S. Ozawa, A. Nishikawa and M. Yoshida, Different pathways of constitutive androstane receptor mediated liver hypertrophy and hepatocarcinogenesis in mice treated with piperonyl butoxide or decabromodiphenyl ether, *Toxicol. Pathol.*, 2013, **41**, 1078–1092.
- 53 Y. Sado, S. Inoue, Y. Tomono and H. Omori, Lymphocytes from enlarged iliac lymph nodes as fusion partners for the

- production of monoclonal antibodies after a single tail base immunization attempt, *Acta Histochem. Cytochem.*, 2006, **39**, 89–94.
- 54 R. A. Irizarry, B. M. Bolstad, F. Collin, L. M. Cope, B. Hobbs and T. P. Speed, Summaries of Affymetrix GeneChip probe level data, *Nucleic Acids Res.*, 2003, **31**, e15.
- 55 W. E. Johnson, W. Li, C. A. Meyer, R. Gottardo, J. S. Carroll, M. Brown and X. S. Liu, Model-based analysis of tiling-arrays for ChIP-chip, *Proc. Natl. Acad. Sci. U. S. A.*, 2006, **103**, 12457–12462.
- 56 M. Bansal, A. Kumar and V. R. Yella, Role of DNA sequence based structural features of promoters in transcription initiation and gene expression, *Curr. Opin. Struct. Biol.*, 2014, **25**, 77–85.
- 57 R. Shippy, S. Fulmer-Smentek, R. V. Jensen, W. D. Jones, P. K. Wolber, C. D. Johnson, P. S. Pine, C. Boysen, X. Guo, E. Chudin, Y. A. Sun, J. C. Willey, J. Thierry-Mieg, D. Thierry-Mieg, R. A. Setterquist, M. Wilson, A. B. Lucas, N. Novoradovskaya, A. Papallo, Y. Turpaz, S. C. Baker, J. A. Warrington, L. Shi and D. Herman, Using RNA sample titrations to assess microarray platform performance and normalization techniques, *Nat. Biotechnol.*, 2006, **24**, 1123–1131.
- 58 M. Schöniger-Hekele, S. Hanel, F. Wrba and C. Muller, Hepatocellular carcinoma–survival and clinical characteristics in relation to various histologic molecular markers in Western patients, *Liver Int.*, 2005, **25**, 62–69.
- 59 H. S. Mohammad, K. Kurokohchi, H. Yoneyama, M. Tokuda, A. Morishita, G. Jian, L. Shi, M. Murota, J. Tani, K. Kato, H. Miyoshi, A. Deguchi, T. Himoto, H. Usuki, H. Wakabayashi, K. Izuishi, Y. Suzuki, H. Iwama, K. Deguchi, N. Uchida, E. A. Sabet, U. A. Arafa, A. T. Hassan, A. A. El-Sayed and T. Masaki, Annexin A2 expression and phosphorylation are up-regulated in hepatocellular carcinoma, *Int. J. Oncol.*, 2008, **33**, 1157–1163.
- 60 G. Min, H. Kim, Y. Bae, L. Petz and J. K. Kemper, Inhibitory cross-talk between estrogen receptor (ER) and constitutively activated androstane receptor (CAR). CAR inhibits ER-mediated signaling pathway by squelching p160 coactivators, *J. Biol. Chem.*, 2002, **277**, 34626–34633.
- 61 X. H. Liao, D. L. Lu, N. Wang, L. Y. Liu, Y. Wang, Y. Q. Li, T. B. Yan, X. G. Sun, P. Hu and T. C. Zhang, Estrogen receptor alpha mediates proliferation of breast cancer MCF-7 cells via a p21/PCNA/E2F1-dependent pathway, *FEBS J.*, 2014, **281**, 927–942.
- 62 H. van Dekken, C. Verhoef, J. Wink, R. van Marion, K. J. Vissers, W. C. J. Hop, R. A. de Man, J. N. Ijzermans, C. H. J. van Eijck and P. E. Zondervan, Cell biological evaluation of liver cell carcinoma, dysplasia and adenoma by tissue micro-array analysis, *Acta Histochem.*, 2005, **107**, 161–171.
- 63 A. Mitselou, D. Karapiperides, I. Nesseris, T. Vougiouklakis and N. J. Agnantis, Altered expression of cell cycle and apoptotic proteins in human liver pathologies, *Anticancer Res.*, 2010, **30**, 4493–4501.
- 64 R. Shizu, S. Shindo, T. Yoshida and S. Numazawa, Cross-talk between constitutive androstane receptor and hypoxia-inducible factor in the regulation of gene expression, *Toxicol. Lett.*, 2013, **219**, 143–150.
- 65 M. Kunz, S. Moeller, D. Koczan, P. Lorenz, R. H. Wenger, M. O. Glocker, H. J. Thiesen, G. Gross and S. M. Ibrahim, Mechanisms of hypoxic gene regulation of angiogenesis factor Cyr61 in melanoma cells, *J. Biol. Chem.*, 2003, **278**, 45651–45660.
- 66 Z. J. Zeng, L. Y. Yang, X. Ding and W. Wang, Expressions of cysteine-rich61, connective tissue growth factor and Nov genes in hepatocellular carcinoma and their clinical significance, *World J. Gastroenterol.*, 2004, **10**, 3414–3418.
- 67 H. Cangul, Hypoxia upregulates the expression of the NDRG1 gene leading to its overexpression in various human cancers, *BMC Genet.*, 2004, **5**, 27.
- 68 J. Cheng, H. Y. Xie, X. Xu, J. Wu, X. Wei, R. Su, W. Zhang, Z. Lv, S. Zheng and L. Zhou, NDRG1 as a biomarker for metastasis, recurrence and of poor prognosis in hepatocellular carcinoma, *Cancer Lett.*, 2011, **310**, 35–45.
- 69 S. Ohnishi, O. Maehara, K. Nakagawa, A. Kameya, K. Otaki, H. Fujita, R. Higashi, K. Takagi, M. Asaka, N. Sakamoto, M. Kobayashi and H. Takeda, Hypoxia-inducible factors activate CD133 promoter through ETS family transcription factors, *PLoS One*, 2013, **8**, e66255.
- 70 S. Yin, J. Li, C. Hu, X. Chen, M. Yao, M. Yan, G. Jiang, C. Ge, H. Xie, D. Wan, S. Yang, S. Zheng and J. Gu, CD133 positive hepatocellular carcinoma cells possess high capacity for tumorigenicity, *Int. J. Cancer*, 2007, **120**, 1444–1450.
- 71 B. Dong, J. S. Lee, Y. Y. Park, F. Yang, G. Xu, W. Huang, M. J. Finegold and D. D. Moore, Activating CAR and beta-catenin induces uncontrolled liver growth and tumorigenesis, *Nat. Commun.*, 2015, **6**, 5944.
- 72 A. Monro, The paradoxical lack of interspecies correlation between plasma concentrations and chemical carcinogenicity, *Regul. Toxicol. Pharmacol.*, 1993, **18**, 115–135.
- 73 M. Assem, E. G. Schuetz, M. Leggas, D. Sun, K. Yasuda, G. Reid, N. Zelcer, M. Adachi, S. Strom, R. M. Evans, D. D. Moore, P. Borst and J. D. Schuetz, Interactions between hepatic Mrp4 and Sult2a as revealed by the constitutive androstane receptor and Mrp4 knockout mice, *J. Biol. Chem.*, 2004, **279**, 22250–22257.
- 74 X. Zhao, Y. Guo, W. Yue, L. Zhang, M. Gu and Y. Wang, ABCC4 is required for cell proliferation and tumorigenesis in non-small cell lung cancer, *OncoTargets Ther.*, 2014, **7**, 343–351.
- 75 D. Feng, Y. Ma, J. Liu, L. Xu, Y. Zhang, J. Qu, Y. Liu and X. Qu, Cbl-b enhances sensitivity to 5-fluorouracil via EGFR- and mitochondria-mediated pathways in gastric cancer cells, *Int. J. Mol. Sci.*, 2013, **14**, 24399–24411.
- 76 A. Iwai, M. Hijikata, T. Hishiki, O. Isono, T. Chiba and K. Shimotohno, Coiled-coil domain containing 85B suppresses the beta-catenin activity in a p53-dependent manner, *Oncogene*, 2008, **27**, 1520–1526.

- 77 R. Yasuhara, Y. Ohta, T. Yuasa, N. Kondo, T. Hoang, S. Addya, P. Fortina, M. Pacifici, M. Iwamoto and M. Enomoto-Iwamoto, Roles of beta-catenin signaling in phenotypic expression and proliferation of articular cartilage superficial zone cells, *Lab. Invest.*, 2011, **91**, 1739–1752.
- 78 A. Al-Sharif, M. Jamal, L. X. Zhang, K. Larson, T. A. Schmidt, G. D. Jay and K. A. Elsaid, Lubricin/Proteoglycan 4 Binding to CD44 Receptor: A Mechanism of the Suppression of Proinflammatory Cytokine-Induced Synovocyte Proliferation by Lubricin, *Arthritis Rheumatol.*, 2015, **67**, 1503–1513.
- 79 C. Bossenmeyer-Pourie, R. Kannan, S. Ribieras, C. Wendling, I. Stoll, L. Thim, C. Tomasetto and M. C. Rio, The trefoil factor 1 participates in gastrointestinal cell differentiation by delaying G1-S phase transition and reducing apoptosis, *J. Cell Biol.*, 2002, **157**, 761–770.
- 80 S. Zhao, Y. Ma and X. Huang, Trefoil factor 1 elevates the malignant phenotype of mucinous ovarian cancer cell through Wnt/ $\beta$ -catenin signaling, *Int. J. Clin. Exp. Pathol.*, 2015, **8**, 10412–10419.
- 81 D. Masson, M. Qatanani, A. L. Sberna, R. Xiao, J. P. Pais de Barros, J. Grober, V. Deckert, A. Athias, P. Gambert, L. Lagrost, D. D. Moore and M. Assem, Activation of the constitutive androstane receptor decreases HDL in wild-type and human apoA-I transgenic mice, *J. Lipid Res.*, 2008, **49**, 1682–1691.
- 82 V. Gonzalez-Pecchi, S. Valdes, V. Pons, P. Honorato, L. O. Martinez, L. Lamperti, C. Aguayo and C. Radojkovic, Apolipoprotein A-I enhances proliferation of human endothelial progenitor cells and promotes angiogenesis through the cell surface ATP synthase, *Microvasc. Res.*, 2015, **98**, 9–15.
- 83 C. Draney, A. E. Hobson, S. G. Grover, B. O. Jack and J. S. Tessem, Cdk5r1 Overexpression Induces Primary beta-Cell Proliferation, *J. Diabetes Res.*, 2016, **2016**, 6375804.
- 84 V. K. Subbaiah, N. Narayan, P. Massimi and L. Banks, Regulation of the DLG tumor suppressor by beta-catenin, *Int. J. Cancer*, 2012, **131**, 2223–2233.
- 85 M. Vinken, E. Decrock, L. Leybaert, G. Bultynck, B. Himpens, T. Vanhaecke and V. Rogiers, Non-channel functions of connexins in cell growth and cell death, *Biochim. Biophys. Acta*, 2012, **1818**, 2002–2008.
- 86 K. Kobayashi, M. Hashimoto, P. Honkakoski and M. Negishi, Regulation of gene expression by CAR: an update, *Arch. Toxicol.*, 2015, **89**, 1045–1055.
- 87 K. Komposch and M. Sibilica, EGFR Signaling in Liver Diseases, *Int. J. Mol. Sci.*, 2016, **17**, 30–60.